

PIONEER PROJECTS

CONSERVATION, IR, UV AND 3D-IMAGING: THE EGYPTIAN EXECRATION STATUETTES PROJECT (EES)

CONTRACT - BR/121/PI/EES

FINAL REPORT

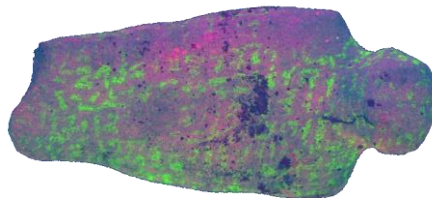
31/03/2017

Promotors

Luc Delvaux (RMAH, Jubelpark 10, 1000 Brussels)
Hendrik Hameeuw (RMAH, Jubelpark 10, 1000 Brussels)

Authors

Luc Delvaux (RMAH)
Hendrik Hameeuw (RMAH / KU Leuven)
Athena Van der Perre (RMAH)
Vanessa Boschloos (RMAH / Ghent University)
France Ossieur (RMAH)
Bruno Vandermeulen (KU Leuven)
Marc Proesmans (KU Leuven)
Dennis Braekmans (TU Delft / Leiden University)





Published in 2017 by the Belgian Science Policy
Avenue Louise 231
Louizalaan 231
B-1050 Brussels
Belgium
Tel: +32 (0)2 238 34 11 – Fax: +32 (0)2 230 59 12
<http://www.belspo.be>

Contact person: Georges Jamart
+32 (0)2 238 36 90

Neither the Belgian Science Policy nor any person acting on behalf of the Belgian Science Policy is responsible for the use which might be made of the following information. The authors are responsible for the content.

No part of this publication may be reproduced, stored in a retrieval system, or transmitted in any form or by any means, electronic, mechanical, photocopying, recording, or otherwise, without indicating the reference :

Luc Delvaux, Hendrik Hameeuw, Athena Van der Perre, Vanessa Boschloos, France Ossieur, Bruno Vandermeulen, Marc Proesmans, Dennis Braekmans. **Conservation, IR, UV and 3D-Imaging: The Egyptian Execration Statuettes Project**. Final Report. Brussels : Belgian Science Policy 2017 – 66 p. (BRAIN-be - (Belgian Research Action through Interdisciplinary Networks)

TABLE OF CONTENTS

CONTENTS

SUMMARY	4
CONTEXT	4
OBJECTIVES	4
CONCLUSIONS	5
KEYWORDS	5
1. INTRODUCTION	6
2. METHODOLOGY AND RESULTS	8
2.1 RESEARCH AXIS 1: CONSERVATIONAL ISSUES	8
2.1.1 <i>The figurines: Inventory and Classification</i>	9
2.1.2 <i>Material study</i>	15
2.1.3 <i>Additional Analyses</i>	20
2.1.4 <i>Conservation and restoration</i>	22
2.2 RESEARCH AXIS 1: MULTISPECTRAL IMAGING	29
2.2.1 <i>Initial tests with Nikon D610</i>	29
2.2.2 <i>The MS PLD Hardware</i>	29
2.2.3 <i>The MS PLD Software</i>	33
2.2.4 <i>The MS PLD Results</i>	37
3. DISSEMINATION AND VALORISATION	48
3.1 TALKS, LECTURES & WORKSHOPS	48
3.2 POSTERS	50
3.3 WEBSITES & BLOGS	50
4. PERSPECTIVES	50
5. PUBLICATIONS	52
6. ACKNOWLEDGEMENTS	53
7. REFERENCES	54
ANNEXES	61
ANNEXE 1: ORIGIN AND DISPERSION OF THE BRUSSELS EXECRATION FIGURINES	61
ANNEXE 2: CONDITION ASSESSMENT FORM	63
ANNEXE 3: WDXRF – RMAH (E.7444).....	65

SUMMARY

Context

The Egyptian collection of the RMAH comprises about one hundred execration figurines made of unbaked clay, bearing curses written in hieratic script (a cursive writing system related to hieroglyphs) and dating to the Middle Kingdom (c. 1850 BC). These represent captured (foreign) enemies and were buried ritually in order to symbolically neutralise foreign and domestic enemies and general threats. Nearly 90 years after their discovery, the red and black pigments used to inscribe these four millennia old objects are now faded or damaged. The Execration texts on these figurines are regarded as one of the most renowned collections of written sources for ancient Near Eastern studies, Egyptian history and Biblical studies for the early 2nd millennium BCE.

When it comes to documenting every characteristic of an object in a highly detailed way, clay artefacts inscribed with ink and other pigments, such as the aforementioned figurines, pose a particular challenge. These three-dimensional media with curved surfaces hold traces of writing that, in some cases, have faded or have disappeared completely. The study of these objects is generally hampered by their poor state of conservation, any handling can result in a considerable loss of material (and therefore also valuable information).

The EES project aimed to develop new imaging techniques (using interactive 2D, 3D and multispectral images) that can improve the legibility of faded inscriptions and enhance the decorations on clay objects. Combining 3D digitisation and multispectral imaging in a user-friendly and transportable system, that is also manageable by curators, conservators, researchers and other stakeholders in the museum, is a truly pioneering project. It must facilitate the management of recorded collections and offer numerous possibilities for historical and art-technical studies on these objects, while the future handling is limited to a minimum, thus ensuring their sustainability.

Objectives

The general objectives of the EES project were:

- To develop a non-destructive and non-invasive recording method for clay artefacts inscribed with ink and other pigments, resulting in virtual models to be visualised and studied with freeware software packages
- To pioneer the abilities of multispectral imaging on clay objects (visible light, infrared and ultraviolet) by using a converted conventional High Definition DSLR camera
- To extend the Portable Light Dome (PLD) system to incorporate additional infrared (IR) and ultraviolet (UV) relighting systems, allowing the output of 3D models with IR and UV based texture maps
- To establish a user-friendly methodology to enhance the visibility of ink and pigment traces on clay objects

- To test this pioneering methodology in a case study, consisting of some 120 Egyptian clay figurines with ink and pigment writings, at different locations

These were extended during the project with:

- A comprehensive analysis of the state of preservation of the figurines, in order to identify and evaluate the factors that may affect the reflection of infrared and ultraviolet light
- A non-destructive analysis of the composition of the clay and pigments with handheld XRF

Conclusions

All the above sketched objectives (initial & additional) were met. Together with the formal partners (RMAH, ESAT-VISICS and Digital Lab – KU Leuven) and with the support of the RICH project – KU Leuven, a multispectral imaging system based on the Portable Light Dome system was developed and tested both on artefacts selected for the case-study as well as on many other archaeological and cultural heritage objects kept at the RMAH and the KU Leuven. Comparison tests with existing state-of-the-art MS systems and techniques have proven the outcome of the new multispectral imaging (MSI) system facilitates the study and improves the legibility of the inscriptions on the Egyptian Execration Statuettes in the line of the other best practise results. In addition, as discussed and presented further in this report, the developed system can also be exploited for research purposes on a broad gamma of various artefacts. The EES project has positioned the RMAH and the KU Leuven with this new kind of research infrastructure in a prominent position to face in the future new challenges in the field of MSI and multi-light/directional reflectance technologies.

Keywords

Multispectral imaging – Conservation techniques – 3D Imaging – IR and UV photography - hieratic texts – ancient geography – Egyptian execration figurines

1. INTRODUCTION

In the summer of 1938, a large collection of figurines was presented to the Belgian Egyptologist Jean Capart by the Parisian antiquarian Joseph Khawam (Bierbrier 2012: 294). The figurines, representing foreign prisoners with bound hands and feet, already spent more than a decade at the antiquarian, when they were acquired by Capart for the Royal Museums of Art and History (RMAH, Brussels) with the financial support of the *Fondation Égyptologique Reine Élisabeth* (the current *Association Égyptologique Reine Élisabeth*) and the *Fondation Francqui* (Van de Walle et al. 1980: 33). These figurines, made of unfired clay and inscribed with hieratic texts, were dated to the Middle Kingdom, based on the palaeography of the hieratic signs. More precisely, the Brussels group is generally dated to the end of the 12th Dynasty, i.e. the reign of Sesostri III or Amenemhat III (c. 1856-1806 BC), or to the beginning of the 13th Dynasty (Posener 1940: 31-35, Ben Tor 2006: 64-66). The content of the texts, comparable to the execration texts on the Berlin Bowls published by Kurt Sethe (1926), identified the figurines as execration figurines. Execration rituals served to offer magical protection against dangerous forces. The focus was on the symbolic destruction of hostile elements (bad things, demons or enemies), represented by statuettes or red pots, often inscribed with the names of the enemies (Ritner 1993: 136-142). An extensive overview of the known Egyptian execration figurines can be found in Posener (1987: 2-6) and Theis (2014: 708-731). The origin and dispersion of the Brussels group is described in Annexe 1. The hieratic inscriptions on the Brussels figurines, written in red and black ink, list the names of foreign places, rulers and/or individual enemies. By focusing on the direct neighbours of Egypt – Libya, Nubia and the Levant – as well as on Egyptian enemies, these figurines are often regarded as crucial primary sources for our knowledge of the political geography of the region. Therefore, they are often entitled as *Prime Cultural Heritage* artefacts. At present, their study is mainly hampered by the poor state of conservation, while a second challenge lies in the only partial preservation of the ink traces, resulting in a great loss of information.

Between 2014 and 2017, the Brussels figurines were the protagonists of the Egyptian Execration Statuettes (EES) project of the RMAH (BRAIN-BE Pioneer: BR/121/PI/EES). This pioneering project focused on the development of a multispectral, multi-light, multi-directional and dome-shaped imaging system, the Multispectral Portable Light Dome (MS PLD), in collaboration with the RICH project (Reflectance Imaging for Cultural Heritage, KU Leuven), the Digital Lab (KU Leuven) and the ESAT-VISICS research group (KU Leuven). The MS PLD uses a combination of Infrared (IR), Red, Green, Blue, Ultraviolet (UV) and 3D images for the conservation and study of small decorated and/or inscribed objects.

Multispectral imaging has already proven its value for the study of manuscripts and palimpsests (cfr. The Dead Sea Scrolls (Caine and Magen 2011), The Archimedes Palimpsest (Easton et al. 2011)). When it comes to using multispectral imaging for the documentation of archaeological objects, the focus lies mainly on papyri and ostraca, i.e. relatively flat objects containing inscriptions and/or drawings (Booras and Seely 1999, Macfarlane et al. 2011, Faigenbaum et al. 2012). In Egyptology, multispectral imaging has also been used for the

documentation of wall paintings (Kotoula 2012), inscriptions on mummy shrouds (Corcoran and Svoboda 2012) and mummy masks and portraits (Ganio et al. 2015). Apart from merely documenting objects, multispectral imaging has also been used for the identification of historical pigments (Dyer and Simpson 2012, Cosentino 2014). Whether there is an actual added value in using multispectral recordings, when simple infrared photography might offer equal results, has been the subject of scholarly discussion as well. The value of MS imaging is questioned by Bülow-Jacobsen 2008, while his statements are countered by Bay et al. 2010.

On the other hand, 3D imaging has been intensively used in the past years. Most satisfying results were reached for reconstructions of large architectural features, objects, paper and canvas documents (e.g. Remondino 2011, Abate et al. 2014) and for the documentation of very small objects or for surfaces on which the smallest details matter, such as archaeological artefacts with cuneiform signs and seal impressions (Hameeuw and Willems 2011). For art conservation, high magnification 3D in-focus microscopy with the HIROX 3D binocular has been explored for examining the surface layers in paintings by Van Eyck, Vermeer, Hals and Van Gogh (Boon 2015).

Recently, photogrammetry and infrared techniques have been successfully combined (i.e. partly integrated) in the study of art and archaeological objects (Bennett 2015, Keats Webb 2015). Furthermore, in isolated test recordings, Reflectance Transformation Imaging (RTI) techniques were used in combination with the use of IR and UV spectra (Kotoula 2012, 2015). Unfortunately, these cases cover only one aspect of the documentation process we are aiming at; the outcome is either a method providing information on the geometry of the recorded surface with a texture map based on visible light, IR or UV separately; or it consists of 2D representations based on a recording process with varying spectral wavelengths whether or not moulded into an integrated interface.

The imaging component of the EES project has in the first place focused on the challenge to (re)visualise the inscriptions on the surface of the figurines. Several sections have faded or even seem completely vanished to the naked eye. Secondly, the fragile condition of the artefacts requires the applied method to be non-destructive, and even more importantly, it must consist of an approach in which handling and physical contact with the figurines can be reduced to a minimum. A third objective is to have a visual documentation system that is capable of registering the physical dimensions of these three-dimensional objects. Taking the latter as a significant requirement, the multi-light, multi-directional reflectance system of the Portable Light Dome (PLD, Willems et al. 2005) was selected as starting point. This acquisition system was further expanded by introducing multispectral imaging techniques, which have been established as being very effective in visualizing features that otherwise cannot be fully distinguished or remain hidden to the naked eye. This not only facilitates the detailed study of these fragile objects, but it also limits their future handling. The system can be widely used for the study of other types of objects, different materials and shapes, thus becoming a valuable tool for future art technical and conservational research.

2. METHODOLOGY AND RESULTS

The project is structured along two parallel research axes, each building on the intermediary results of the other allowing to make the necessary modifications during the process. While one axis focuses on the multispectral imaging and the development of the MS PLD system, the other centres on the condition of the figurines and their surfaces to be recorded by this system and to be studied by archaeologists, epigraphists and art historians. Every characteristic of the selected objects needs to be meticulously studied, including their chemical composition, the used conservation products and the production method, since these can influence the reflectance characteristics and therefore the output of the recording sessions.

The progress in the development of the new technologies behind the MS PLD has been reported through the publication of several case studies (Van der Perre and Hameeuw 2015, Watteeuw et al. 2016, Van der Perre et al. 2016), while the results of the conservational assessment exercises are presented in Van der Perre et al. (forthcoming) and the chemical analyses in Braekmans et al. (forthcoming).

2.1 Research axis 1: Conservational Issues

An initial phase of the project consisted of establishing a condition report of the entire Brussels group. By setting out from an inventory of the figurines and the fragments in the Egyptian department's storerooms and exhibition halls, 104 objects were identified, of which 31 complete and 73 incomplete. Three small coffins, made of unfired clay, also belong to the assemblage. The inventory was combined with a typological classification and with a classification into conservational categories. The typological study was undertaken based on the technological aspects of the figurines' manufacture and on their general appearance. They show potential as well for palaeographical classification, since several handwritings can be distinguished in the inscriptions (Posener 1939: 41).

In addition, X-Ray Fluorescence (XRF) analyses of all items offered insights into the composition of the clay and allowed identifying groups. Especially the composition of the pigments used to inscribe the figurines and their state of preservation helped determining imaging parameters for the MS PLD.

The conservation study was multifocal: for each individual figurine a condition assessment form was filled out with a selection of criteria based on the preliminary examination of the entire group (Annexe 2). An initial assessment under a magnifying lamp was completed with observations made by means of a trinocular microscope (Leica M80 with 8:1 zoom range and magnification of 7.5x-60x). Their state of preservation was assessed and described in detail and previous consolidation and restoration interventions were identified.

2.1.1 The figurines: Inventory and Classification

Types

At first sight, the RMAH collection contains two groups: large figurines (> 30 cm), carrying the nearly complete version of the execration texts (including references to non-Egyptian enemies), and a second group of smaller figurines (c. 10-15 cm), carrying references to Egyptian individuals and 'negative things' in general. Based on the research conducted during the project, this rough division was refined into five types, Types A-E, of which E contains two subtypes (E1-E2) (Table I). In a number of cases, it was not possible to define the exact subtype due to an only partial preservation of the figurine. Since all figurines originated at Saqqara, it is possible that each type represents the hand of an individual craftsman.

Large figurines (Type A)

The first type includes all large figurines (with an average length of c. 30 – 35 cm), depicting a foreign prisoner, seated on his knees, with his arms and feet bound together on his back. Although the finishing of the body is very rudimentary, the head has been very carefully sculpted. The typical characteristics of the enemies of Egypt were emphasised, as it was important that they were unmistakably recognisable (Capart 1939: 68-69).

The arms are not modelled separately, but the external contours are marked by low relief on the back of the figurine, dividing it in four parts. On the majority of these large figurines a hole can be observed in the central part of the back, under the elbows. It appears that these holes were used to bind the modelled arms together with a string. Carbonised fibres, traces of friction, and imprints of strings confirm that the holes were actually used for this purpose (Posener 1940: 18-19).

The hieratic inscriptions were made with ochre paint, carefully written in a small and well-cared handwriting. These long inscriptions contain the complete version of the Execration Texts, including all sections (A-P) presented by Sethe in his publication of the Berlin bowls (Sethe 1926: 32-72). The Brussels version, however, contains a more elaborate list of foreign cities and rulers. Given the importance of this information for the study of the geographical and political history of Middle Kingdom Egypt and its neighbours, Posener rapidly published the Asian and Nubian lists in *Princes et pays d'Asie et de Nubie* (Posener 1940).

Small figurines (Types B-E2)

Remarks on the inventory cards of the RMAH suggest that Posener selected five major types (Séries I-V), which were divided into subtypes. However, these remarks are not present on every form, and at this moment, we do not have access to his personal notes. The results concerning his study on the smaller figurines were never published, so many questions remain unanswered. The EES project proposes a new division of the small figurines, resulting in four types, dubbed Types B to E.

As can be seen in Table I, the majority of the Brussels group consists of small figurines. These figurines are c. 10-15 cm, roughly modelled and lack a detailed rendering of facial features. The head is hardly marked, as are the legs. Since the figurines are clearly handmade without the use of moulds, this often results in differences in the height of the shoulders, or the width of the modelled legs. In order to create the head, an additional lump of clay was added (e.g. E.7459). Some figurines appear to have a crudely modelled wig on the head.

All figurines bear either ochre or black hieratic inscriptions. The direction of writing could alter. Horizontal lines of text were either crossing the figurine from one side to the other, or were written from top to bottom. Although the majority is inscribed on both sides, a number of figurines only bears inscriptions on the front (recto). These texts cannot be categorised as the standard execration texts, known from the Berlin bowls, but are connected to the earlier (and later) inscriptions found on execration figurines (e.g. Quack 2002). They refer to individuals -mainly Egyptians-, mentioning their affiliation, generally including both the mother and the father. An individual is often specified by its nickname, using the expression *Dd.w n=f*, “He who is called”. In rare cases, the texts do not refer to persons, but to “bad” things and habits in general.

Some of the smaller figurines have been buried in roughly made, miniature coffins (Capart 1939: 69). Three coffins are currently stored in the RMAH: E. 7493b, E.7494b and E.9101. Only the last one is on display.

TABLE I: Execration figurines divided into types

Type A	Inv. N°
	E.7440, E.7441, E.7442, E.7443, E.7444
	E.9060, E.9061, E.9062, E.9063, E.9064
	E.9095
	E.7442

Type B

Inv. N°



E.7445, E.7446, E.7447, E.7448, E.7449
 E.7451, E.7472, E.7489, E.7490, E.7491,
 E.7492
 E.7608, E.7611, E.7614
 E.9076, E.9079, E.9090, E.9092, E.9093

E.7491

Type C

Inv. N°



E.7452, E.7454, E.7463, E.7466
 E.7607, E.7610, E.7613
 E.9071, E.9082, E.9083, E.9084, E.9085,
 E.9086
 E.9091, E.9094, E.9097, E.9100

E.7454

Type D

Inv. N°



E.7453, E.7458

E.7453

Type E1

Inv. N°



E.7450, E.7455, E.7456, E.7460, E.7461,
 E.7462, E.7464, E.7465, E.7467, E.7468,
 E.7469, E.7471, E.7473, E.7474, E.7477,
 E.7478, E.7479, E.7480
 E.7484, E.7493, E.7494, E.7612
 E.9065, E.9066, E.9067, E.9068, E.9069,
 E.9077, E.9078, E.9080, E.9081, E.9088,
 E.9096

E.7462

Type E2**Inv. N°**

E.7457, E.7459, E.7470, E.7475, E.7476
E.9070, E.9073, E.9075



E.7459

Type E1/E2**Inv. N°**

E.7468, E.7481, E.7482, E.7483, E.7485,
E.7486, E.7487, E.7488, E.7609
E.9072, E.9074, E.9087, E.9089, E.9098,
E.9099

Manufacturing techniques

As stated above, the figurines of the RMAH are made of unfired clay and inscribed with hieratic texts. They are clearly hand-modelled, no evidence for the use of moulds can be found, but there are some noticeable differences in the manufacturing techniques. This was confirmed by visual observations and experimental production of several figurine types by the RMAH's ceramics conservation lab, under direction of France Ossieur. The recreation of the figurines confirmed that no tools were used during the production, all marks and features were made with bare hands, using hand, fingers and fingernails to shape the figurine and its physical details. This is clearly demonstrated in Fig. 1, comparing our newly made figurines to the originals. The experiment established the small figurines were modelled from a single clay roll or coil. The traces left behind by fingers smoothing the surface are almost identical on both the original and the modern hand-modelled figurine. Generally, the head was not added but shaped by pinching the clay between the shoulders. On some occasions, however, a small amount of clay was added to give more volume to the face.

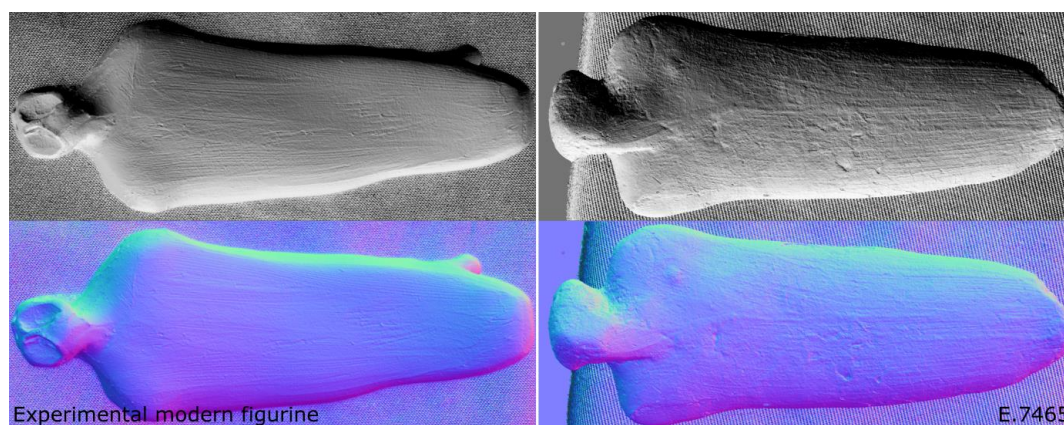


Figure 1: Comparison between figurine E.7465 (right) and a modern copy (left); recordings made with the PLD system, above visualised without colour filter, below with the normal filter (© KMKG-MRAH; Portable Light Dome).

The only exceptions are the holes made on top of the head of the large figurines, where a pointed utensil (organic or metal) must have been used given their regular outlines. A tool was also used to engrave the arms on the back of figurine E.7476.

Surface treatment: Wet-finish or slip

The figurines have been smoothed after being modelled in order to facilitate the writing of the inscriptions. The majority of the figurines has a wet-finish (also called wet-smoothing or self-slip) (Fig. 2a). The creator of the figurine dips his hands in water and subsequently runs his fingers over the surface to smoothen it (Arnold and Bourriau 1993: 85-86). A distinct, thin layer is thus created on the object, consisting of fine clay particles and water, often showing traces of (partial) fingerprints (Fig. 2b).



**Figure 2: a) Traces of wet-finishing on the surface of figurine E.7471 (recto);
b) Traces of fingerprint between the feet of E.7491 (© KMKG-MRAH).**

The traces are documented in the finest detail on the MS Dome recordings, including the direction of traces and the depth of the marks (Fig. 3). The quantity of water used for this technique influences the current state of preservation, because this layer is often a very fragile part of the figurine, as will be discussed below.

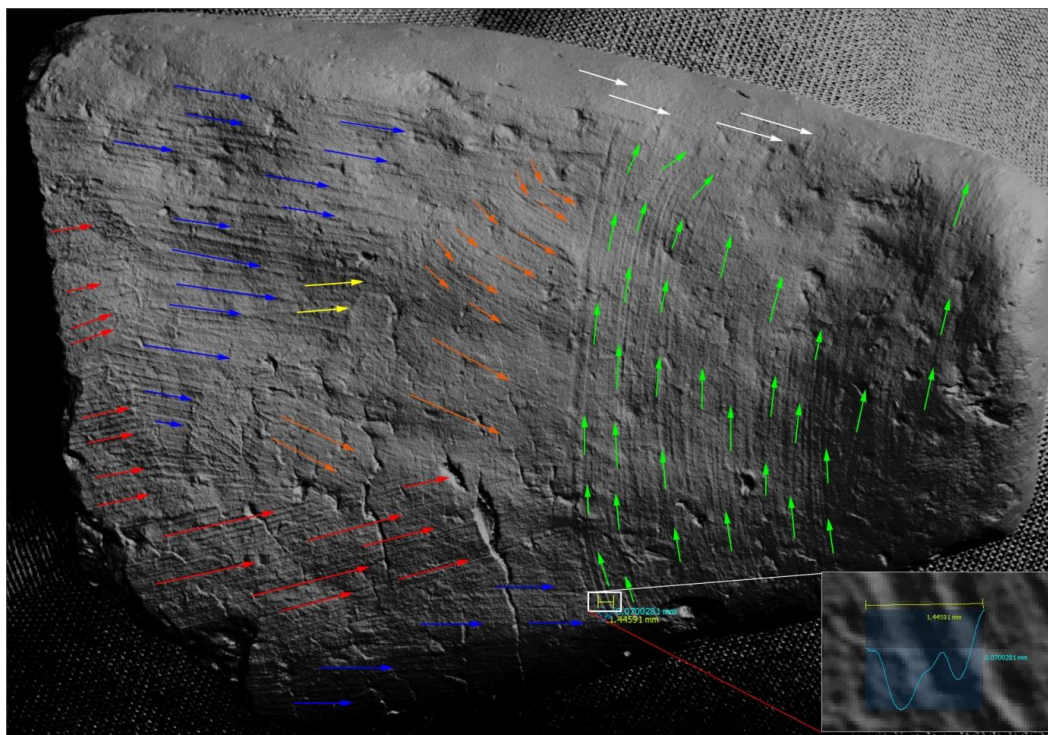


Figure 3: Directions of smoothing marks by fingers on the surface of E.7453 (recto), PLD viewer in shaded exaggerated mode (©KMKG-MRAH & KU Leuven).

As is presented in Fig. 4, this smooth layer is not applied all over the surface of every figurine, but always to the front and often continued to the sides (evidence found on 93 out of 104 figurines). It must be noted that on three figurines the layer does not continue on the right side, and on three others it cannot be discerned on the left side. It was, however, rarely applied to the back of the figurine: only 18 figurines show traces of (partial) wet-finish on the back, even though the figurines often contain inscriptions on the verso. Interestingly, some of these figurines with a wet-smoothed back, do not bear inscriptions on that side at all, raising the question whether the person smoothing the surfaces knew beforehand how much text was going to be written on the figurine and, subsequently, whether this is evidence for a specific *chaîne opératoire* in the manufacturing of the execration figurines.

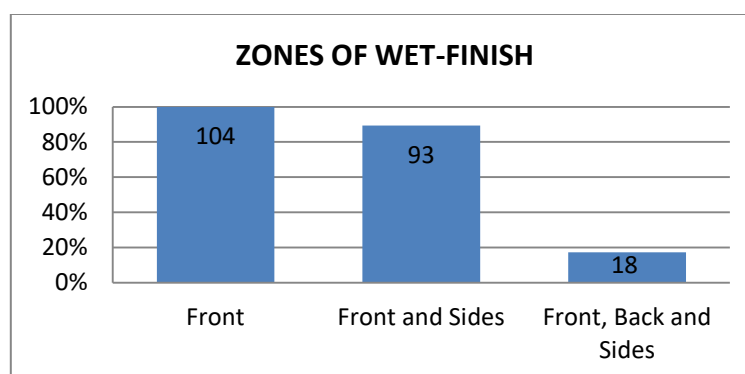


Figure 4: Graph showing the number of execration figurines per zone that received a wet-finish layer.

Certain figurines (E.7454, E.9083, E.9087) show traces of a white layer, apparently applied before the inscription (Fig. 5). Initially it was thought to be a white slip layer or *engobe*, a mixture of clay of a different colour suspended in water. Further research however, has shown that it is not a slip layer, but merely a crystallisation of salts causing a paler appearance of the wet-finished surface.

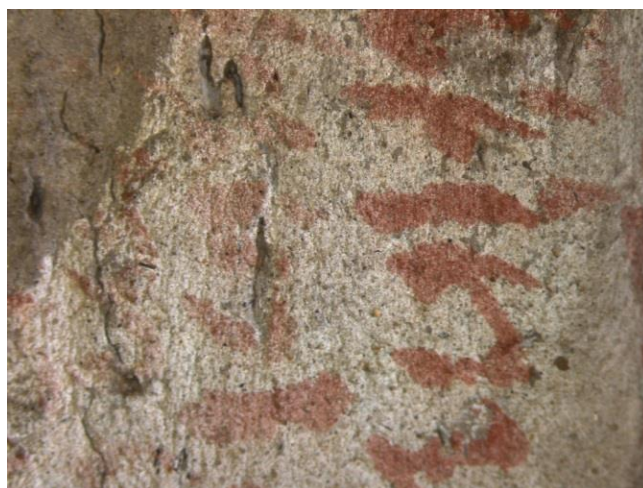


Figure 5: Detail of figurine E.7454 (verso) showing traces of a white layer, photograph made with Leica trinocular (© KMKG-MRAH).

2.1.2 Material study

Clay

The precise type of clay is currently being determined, the results will be published in Braekmans et al. forthcoming. Based on the general appearance of the clay, it is likely that a Nile silt was used. Nile silt and marl clays are the two most common raw materials of pottery manufacture in ancient Egypt (see: Bourriau et al. 2000: 121-122). The colour of the clay has Munsell codes 5YR 5/1-5/2-5/3. Nile silts have been deposited by the river, are rich in silica and iron, and appear grey to black in their raw state. Marl clays are calcareous and rich in mineral salts. These salts often cover the surface of the objects in a thin white layer, easily mistaken for a deliberate “slip” coating (Bourriau et al. 2000: 121-122). Both Nile silts and Marl clays were used throughout the Pharaonic period in the entire Nile Valley.

Whereas Egyptian pottery can be classified according to the Vienna System, currently regarded as the standard classification system for Egyptian ceramics, this is not applied to the raw materials, i.e. the unfired clay. Based on the quantity of, and variation in the inclusions, the composition of the clay suggests that the figurines’ clay might be categorised as Nile B2, or even Nile C, rather than a marl clay. Nile B2 mainly contains sand, medium-sized limestone particles and straw. The Nile C fabric generally includes plant remains, ash, bone, shell, limestone and sand (Bourriau et al. 2000: 130-131; Wodzinska 2009: 21). Marl clay, however, contains very few organic inclusions (Arnold and Bourriau 1993: 166).

The main problem in using these categories lies in the fact that the raw material and the fired pottery are not directly comparable. The processing of the pottery has changed its elemental and mineralogical composition. No reference collection of raw clay of the Saqqara area is currently available. Furthermore, no (archaeological) evidence has been found concerning the figurines' precise production area or clay source.

The question arises whether the clay of the figurines has been processed or not. The figurines contain several (large) inclusions that can be identified with the naked eye, suggesting a temper might have been added to the raw material. Mineral inclusions are present in all figurines, while a large number contains inclusions of ashes and organic material, sometimes carbonised. Reed particles, chaff, carbonised barley, wood splinters are all very common, even remnants of small (grape) and large seeds (*fabaceae* family) were discerned. The botanical remains in figurines E.7443, E.7456, E.7471 and E.7614 were examined by macro stereoscope. Small voids in the clay suggest the degradation of organic inclusions, or these voids might indicate an irregular drying rate, suggesting a complete lack of preparation and blending of the clay. A large number of small, grey-white granules can be discerned, they may be identified as limestone particles but require further analyses. Crushed sherds were definitely added to the raw clay, this is a typical temper for Nile B2 (Arnold and Bourriau 1993: 163), but while in some figurines their presence is only suggested by small orange-brown inclusions, other figurines contain large sherds (c. 2 cm on Fig. 6). Although the identification is often hard, several figurines clearly contain shell fragments (Cf. Fig. 7), thus suggesting the presence of a Nile C fabric (Arnold and Bourriau 1993: 163).



Figure 6: Full view and details of figurine E.7456 (recto) showing large inclusions, such as a sherd (a) and a pod of an Acacia (*fabaceae* family) (b) (© KMKG-MRAH).



Figure 7: Detail of figurine E.7454 (head) showing shell inclusion, photograph taken with Leica trinocular (© KMKG-MRAH).

Preliminary results indicate a relative homogenous production and resource utilisation of these figurines. Nevertheless, few figurines show considerable variation, indicating a different source of clay raw materials – or at least a fundamental different technological approach in the production process (Fig. 8). An explorative study into the possibilities and a provenance assessment of these objects is the scope of a forthcoming paper (Braekmans et al. forthcoming).

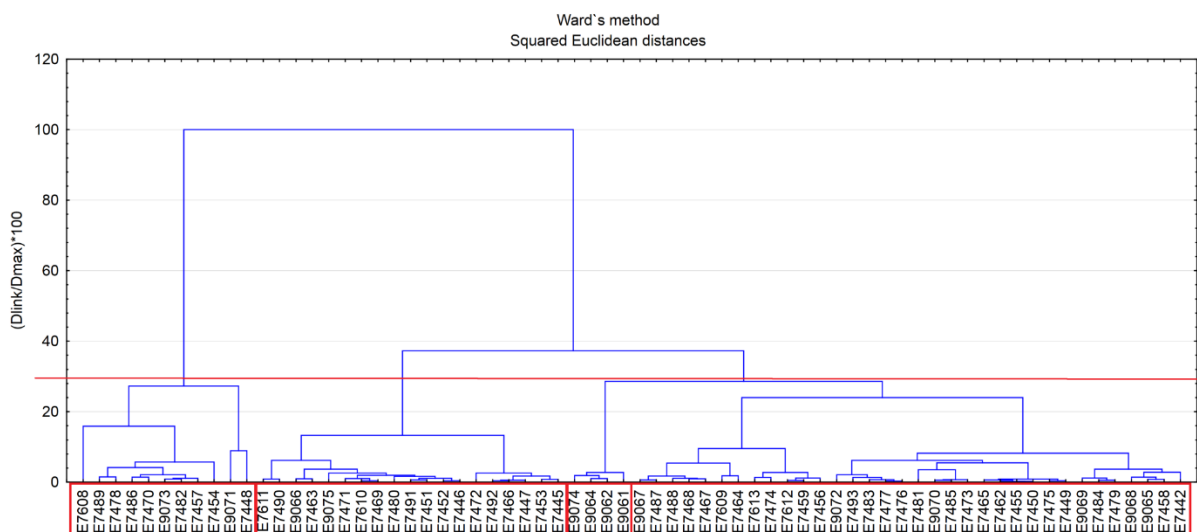


Figure 8: Hierarchical cluster diagram utilizing squared Euclidean distances and Ward's method algorithm. This graphical representation of (dis)similarity in the bulk geochemical composition of the figurines show at least two, potentially three, main geochemical signatures.

A WD-XRF analysis was conducted on a powder sample (saved and labelled during a conservation action in the past) of E.7444. The measurements of the analysis are reported in Annexe 3 and will be discussed in Braekmans et al. forthcoming.

Pigments

Two types of pigments were used: black and red. These colours were, first of all, the standard colours on an Egyptian writer's palette (Lee and Quirke 2000: 117-118). However, the use of certain colours in ancient Egypt also has a magical connotation. Red is often (negatively) associated with Seth, the god of disorder and violence, and underworld demons (Ritner 1993: 147-148, Pinch 2001: 182-185). The colour black, however, does not have these strong negative connotations. It is associated with the darkness of the underworld, but also with the fertile Nile silt and the resurrection of Osiris (Blom-Boër 1994: 57, Pinch 2001: 183). The latter colour is (therefore?) less present on the figurines; 10 figurines are inscribed with a black pigment whereas 94 carry red inscriptions.

The explorative approach for the pigments by HH-XRF entails a purely qualitative approach. By direct comparison of spectra obtained from both pigment-rich and pigment-poor parts of the ceramic, a potential differentiation can be documented, directly connected to a variation in surface composition.

The measurements were evaluated by an assessment of absolute spectra through the use of supplementary software provided by the manufacturer (S1XRF and ARTAX) (Fig. 9). While the obtained spectra are consistently similar, variation was observed in Fe content in the red coloured parts (Fig. 10). Analysis was conducted on objects E.9068 (red), E.7610 (red), E.7489 (black) and E.7450 (two types of red). An analysis of Rh normalised ROI data further confirm this observation (Fig. 11). Apart from the difference in Fe content no other elements show anomalous compositions compared to the general ceramic. The Fe enrichment might point at the utilisation of red ochre (due to hematite) for these red pigments. There is no identification possible or any elemental enrichment detected in the other elements. Either the applied colours are too thin or are composed of organic based materials, which cannot be detected with the equipment used here. Based on these explorative results, higher resolution equipment might further clarify the nature and composition of the observed pigments.

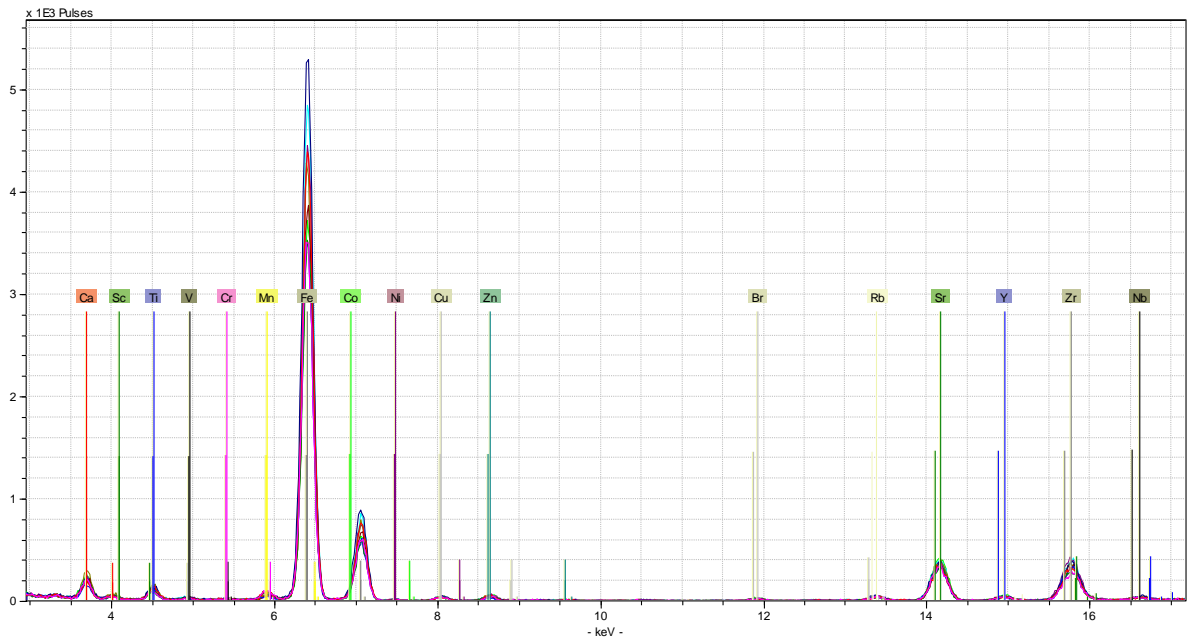


Figure 9: Graph of all spectra indicating the detected elements: Ca, Sc, Ti, V, Cr, Mn, Fe, Co, Ni, Cu, Zn, Rb, Sr, Y, Zr and Nb.

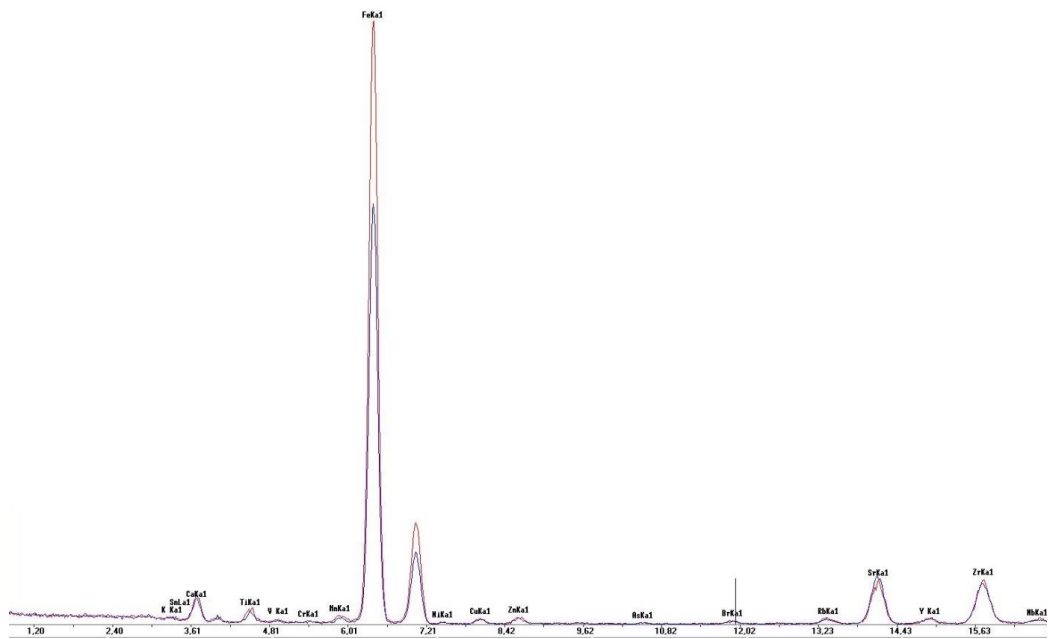


Figure 10: Spectrum with direct comparison between red pigment measurement (red) and non-coloured part of the ceramic (blue) (figurine E.7610).

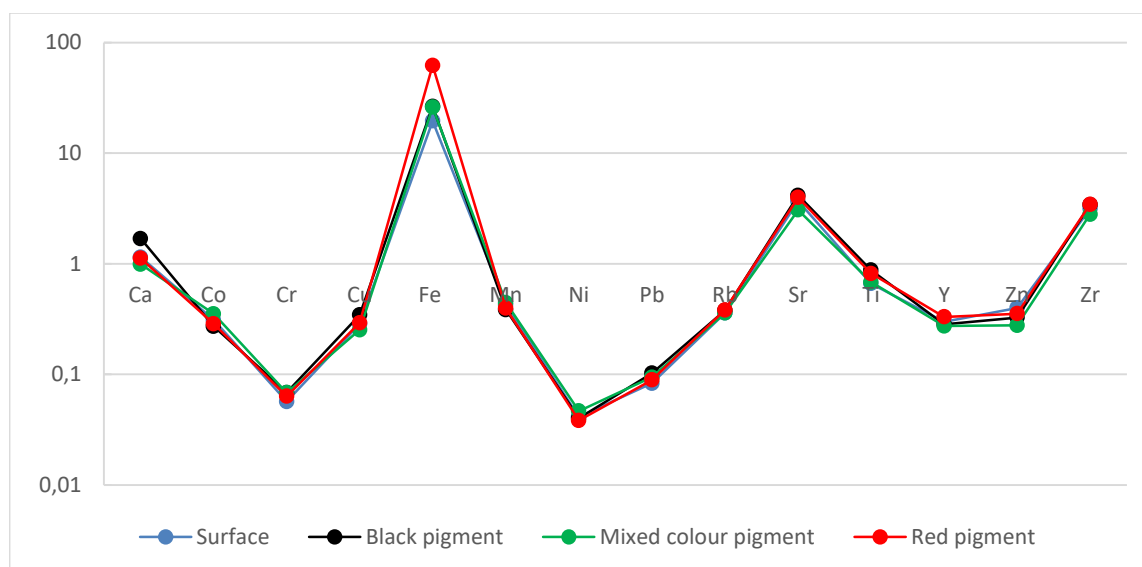


Figure 11: Rh normalised counts per second spider plot indicating elemental variation (logarithmic scale).

2.1.3 Additional Analyses

KIK-IRPA & UGent

The observations of the HH XRF equipment are consistent with data obtained from higher resolution equipment. As a reference, figurines E.7459 (red pigment) and E.7614 (black pigment) were analysed with the Bruker Large Area Micro XRF Spectrometer M6 Jetstream of the Royal Institute of Cultural Heritage (KIK-IRPA) in Brussels (Fig. 12). Measurements were taken in air for 40 seconds, using a $150\mu\text{m}$ spot size and a distance of $125\mu\text{m}$ between two measurements (E. 7459 and E. 7614). Measurements on figurine E.7459 were also taken in air for 20 seconds, using a $500\mu\text{m}$ spot size and a distance of $450\mu\text{m}$ between two measurements. The figurines were also tested with Micro-Raman Spectroscopy at the KIK-IRPA. The combined results of both tests confirm the identification of carbon black, but did not give any decisive answer concerning the red pigment. The XRF-mapping provided no added value in the detection and potential visualization of the faded remnants of the pigments (black and red). The technique was unable to differentiate in the computed visualizations the zones with and without pigment traces.



Figure 12: Figurine E.7614 undergoing Large Area Micro XRF analysis (photograph by H. Hameeuw).

Figurine E.7489 (black pigment) was also tested with Raman mapping at the Raman Spectroscopy Research Group (Ghent University) during the Spring of 2017 (Fig. 13). The results, however, were very meagre. The mapping was able to detect the pigment traces still visible with the naked eye; but no seriously faded pigments were detected. It must be concluded that either these faded parts of the inscriptions did not contain enough pigment to be reconstructed by the Raman mapping, or the spot size of the measurements were too large for the potential remnants.



Figure 13: Figurine E. 7489 during Raman mapping at Ghent University (photograph by H. Hameeuw).

2.1.4 Conservation and restoration

For each individual figurine a condition assessment form was filled out with a selection of criteria based on the preliminary examination of the entire group (For an example of this form, see Annexe 2). An initial assessment under a magnifying lamp was completed with observations made by means of a trinocular microscope (Leica M80 with 8:1 zoom range and magnification of 7.5x-60x). Their state of preservation was assessed and described in detail and previous consolidation and restoration interventions were identified.

Conservation reports

Due to their fragile condition, a vast amount of the figurines underwent conservation or restoration treatments, the most recent in 1997-1998. However, these interventions have hardly been documented. The inventory file of E.7494a mentions that the figurine has been treated in a laboratory and that this was documented in “rapport 27/8/51”. Restorations during the 1950s took place in the Royal Institute for Cultural Heritage (KIK-IRPA Brussels). The file, however, only concerns the restoration and conservation of the small coffin (E.7494b) that originally contained figurine E.7494a (Brussels, KIK-IRPA, dossier 1950.00667). The only figurines having an actual report on treatments they received in the late 1990s are E.7441, E.7444, E.7448, E.7472 and E.7480.

This lack of documentation is causing several problems for conservators, curators and researchers working with the figurines. For this reason, a condition report form was drawn up by the present authors. It contains the following categories: general information on the object (e.g. present location, photographs...), condition of the surface layer, information on the inscriptions, condition of the interior, and a separate section on previous conservation and restoration treatments. The form was completed for each figurine. No chemical analyses were conducted to further identify consolidation or restoration products.

Damage and threats

When describing the main issues concerning the conservation of the figurines, it is clear that a distinction needs to be made between the surface and the interior of the figurine. Most preservation issues seem to be related to the composition of the raw clay and the quantity of water used during the manufacturing.

The number of problems occurring in the interior of the figurines is fairly small. Generally this is limited to cracks and crazing, making the figurine structurally unstable (Fig. 14). This can often be directly linked to the composition of the clay, especially to the size and number of inclusions. On the other hand, these cracks can penetrate fairly deep into the inner structure of the clay; presumably the result of the manufacturing procedure causing the surface layer to bound firmly with the clay body. As a consequence, with this particular manufacturing procedure - most probably related to the amounts of water used throughout the modelling and the wet-finishing -, time had a more severe impact on the entire integrity

of these figurines, especially when compared to those for which most of the damage only occurred on the outer shell (Cf. Fig. 15). Moreover, figurines are often broken at the neck. This might be a consequence of the manufacturing process, during which an additional piece of clay could be added to the head to give more volume to the face, thus creating a weaker connection between the head and the body, particularly on the large figurines. Previous restorations include reassembling the broken figurines by using an all-purpose glue (based on the few available treatment reports this can be identified as Velpon) or a mixture of clay and wood glue.



Figure 14: Cracks and crazing observed on figurine E.9097 (© KMG-MRAH).



Figure 15: Problematic cohesion of surface layer with clay body of figurine E.7447 (© KMG-MRAH).

The inscriptions are mostly damaged by the flaking off of the wet-finish surface layer (Cf. Fig. 15). This is caused by the fact that the original structure of the clay has been changed due to the water and smoothening, creating a thin layer that reacts differently to the drying process than the rest of the clay mass. It has the tendency to easily detach itself from the clay body, especially when salts are being formed. Intervention reports mention that, a few decades ago, conservators tried to halt this degradation process by treating the most problematic surfaces with a varying percentage of an acrylic resin, Paraloid B-72, diluted in Paraxylene. The product was either applied locally (Fig. 17) or the entire object was submersed in it. Percentages from 4% up to 7 or 9% Paraloid will darken the clay, whereas a satin shine can be observed on all treated figurines.

It must also be noted that the wet-finish layer has flaked off on those parts of the figurine containing large inclusions. This is clearly visible on Fig. 6, where the sherd and the large pod were originally covered by a very thin layer of wet-finish, which did not stand the test of time. It can also be observed on the wood splinter inclusion in E.7471 (Fig. 16), where remains of the pigment are still visible.



Figure 16: Detail of figurine E.7471 (proper right side) showing a wood splinter inclusion. Remains of the thin wet-finish layer are visible on top of the wood splinter, including some very small traces of pigment (© KMKG-MRAH).

Other problems threatening the inscriptions are the cracks formed in the interior of the figurine, but continuing to the surface. The presence of salts on the surface or the use of consolidation products causing discolouration of the pigments also hamper the readability of the inscriptions. Likewise, stains of glue from old labels or restorations, have caused inscriptions to discolour or fade completely.



Figure 17: Local surface consolidation with acrylic resin on figurine E.7441 (verso), detail photographed with Leica trinocular (© KMKG-MRAH).

Small black spots can be observed on the surface of the majority of figurines (i.e. on 85 of 104 figurines) (Fig. 18), in some cases clustering to large stains. Their identification as manganese dioxide accretions is likely. Those are formed by bacteria, as a result of water seeping through the soil in which the objects were buried. Basically they are the result of a corrosive reaction occurring when manganese is oxidised to MnO (O'Grady 2005; Casaletto *et al.* 2008; Serotta 2010).



Figure 18: Detail of figurine E.7613 (recto) showing black spots, presumably manganese dioxide accretions (© KMKG-MRAH).

Conservation categories

With this assessment, the collection has been divided into four conservation categories, based on the current condition of the surface layer and of the interior, and on their mutual cohesion. The figurines were also compared to the original black and white photographs.

Although we do not know the exact date on which these were taken, the available evidence suggests that this took place fairly soon after their arrival and definitely before 1946, when five additional figurines arrived (See Annexe 1). These are the only figurines without black and white photographs.

Category 1:

- Condition interior good
- Condition surface layer good

48 figurines could be placed under this first category; they are labelled as being stable. There are no or little clear damages, no signs of active deterioration or other observable threats. No urgent conservation recommendations are needed, nor are other (immediate) actions required.

Category 2:

- Condition interior good
- Condition surface layer bad/problematic

The second category houses the figurines of which the internal structure is considered stable, but where the condition of the wet-finish layer is problematic. Since the surface layer contains the inscriptions, a regular inspection is required. In some cases a treatment is desirable, in order to stabilise the object. Currently, 21 figurines have this condition; for some the surface layer has completely decomposed or flaked off (e.g. Fig. 19), for others that process is limited to particular zones (e.g. Fig. 15).



Figure 19: Figurine E.7460 (recto). Left: Original photo (before 1946). Right: Current condition. The wet-finish layer has completely disappeared (© KMKG-MRAH).

Category 3:

- Condition interior bad/problematic
- Condition surface layer good

When the cohesion of the clay body is of a low quality, but the surface is still (almost completely) intact, the object is assigned to Category 3 (Fig. 20); 12 figurines received this label. The condition of the interior directly influences the state of preservation of the inscriptions, and therefore, a regular inspection of the objects is required.



Figure 20: Fragment of a large figurine (E.9061), with well-preserved surface layer but unstable interior. Left: original photograph (before 1946), Right: current condition (© KMKG-MRAH).

Category 4:

- Condition interior bad/problematic
- Condition surface layer bad/problematic

The fourth category comprises all objects being in a deplorable state (E.g. Fig. 21). They were the main reason for choosing the Egyptian execration figurines as case-study for this project. 23 figurines had to be categorised in this section. Obviously, immediate action is required.



Figure 21: Figurine E.7448 (recto). Left: original photo (pre-1946). Right: Current condition. Parts of the head, the shoulders and the wet-finish layer are missing and the interior structure is unstable (© KMKG-MRAH).

The overall result of dividing the entire collection in conservation categories is shown in Fig. 22. Less than half of the figurines are currently in a stable condition, the majority of the figurines show signs of significant retrogression or a problematic state of preservation. During the assessment, it became clear that 39 figurines show signs of active deterioration, either on the surface or internal. Unnecessary handling and transportation of the figurines, especially those in conservation categories 2, 3 and 4 is strongly discouraged.

CONSERVATION CATEGORIES

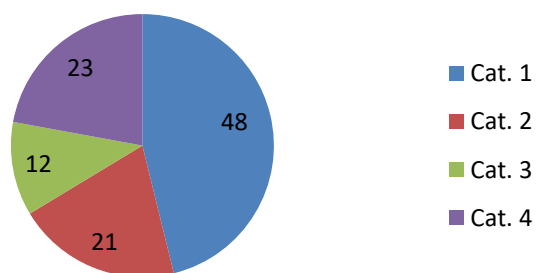


Figure 22: Number of figurines in each conservation category.

This multifaceted approach allowed categorising the factors that influence the legibility of the figurines and thus provided the necessary feedback for the development and adaptation of the MS PLD, described in the following section.

2.2 Research axis 1: Multispectral Imaging

2.2.1 Initial tests with Nikon D610

The firsts images of the execration figurines were made in the Digital Lab (KU Leuven) with a converted Nikon D610, of which the UV-IR filter was removed. Preliminary tests were made with nine UV-IR camera filters (PECA 900-918), using three types of lights (Blacklight UV, Tungsten and Elinchrom) and the CoastalOpt 60 mm UV-VIS-NIR lens.

It was clear that, although our approach clearly worked, some of the obtained images often needed secondary processing in Capture One before the inscriptions on the figurines were sufficiently enhanced. Since the project's ambition was to enhance the inscriptions without additional processing, we had to select the filters that gave the best results. By comparing the test images made with the individual filters and under different lights, the ideal spectra were determined. The following spectra were selected: UV 365nm, Blue 460 nm, Green 523 nm, Red 623 nm, IR 850 nm.

For those objects that do not fit under the PLD, the EES project has chosen to convert a Nikon D810 camera (36.3 MP) by removing the UV-IR filters.

2.2.2 The MS PLD Hardware

The starting point was the initial hard- and software infrastructure of the Portable Light Dome system (Willems et al. 2005), which is continually evolving into an effective tool for studying, monitoring and understanding the materials and surface characteristics of a wide variety of heritage objects (Hameeuw and Willems 2011; Watteeuw et al. 2013). The initial outcome of the PLD system was the 'Minidome' with 260 white light (VIS) LED emitters (Ø80x80mm); transformed within the RICH project into a smaller Microdome with 228 white LEDs (Ø30x30mm). The combined multispectral efforts of RICH and EES resulted in a MS Microdome (finished) and a larger MS Minidome (Fig. 23, under development).

Based on the experiences gained throughout the development stages and thanks to the joint input by heritage specialists, archaeologists, art historians, epigraphists, photography experts and electrical engineers, the multispectral component could be incorporated into the existing PLD system.

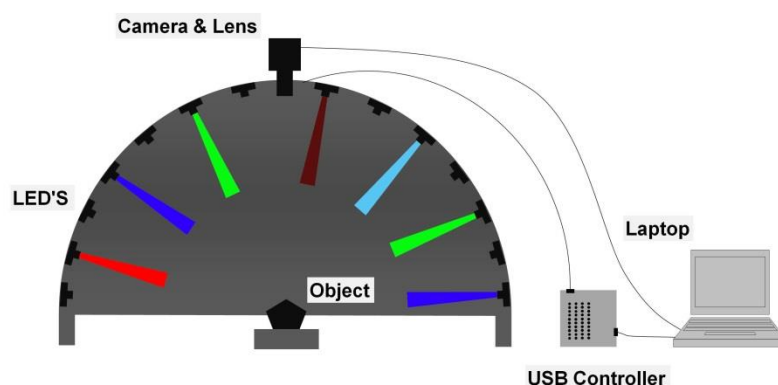


Figure 23: PLD system “Minidome” set-up (© KMKG-MRAH & KU Leuven)

Within the RICH project, the white light Microdome was specifically adapted towards documentary heritage objects such as manuscripts and books. To allow for the imaging of the interior, fragile bookbinding of manuscripts, a segment of the Microdome can be taken off. A rigid structure on top of the dome hosts the high-resolution sensor (28.8 million pixels) and lens combination. It also allows the Microdome to fit onto a Conservation Copy Stand (developed by Manfred Mayer, Graz) as well as a standard tripod or studio stand. Therefore the Microdome can be used in many desired positions or angles (e.g. Fig. 24).



Figure 24: Imaging a decorated yellow coffin from the Egyptian collection of the RMAH: MS Microdome on tripod (© KMKG-MRAH)

Sensor

The sensor of choice is the Allied Vision Prosilica GX 6600. It is a high-resolution 35mm machine vision CCD sensor (6576 × 4384 pixels) enabling vibration free capture through the digital shutter, the latter as opposed to a manual shutter. The resolution of the sensor allows for the capture of small details at high magnification factors. The sensor can be delivered in both a colour and black and white version. The black and white sensor is sensitive in the UV, visible and IR spectra. The colour version has been fitted into the white light Microdome, the black and white version into the multispectral Microdome.

Lens

Ultraviolet and infrared light have a different plane of focus than visible light, an effect also known as 'focus shift'. The PLD uses all the LEDs, with their different light spectra, within one and the same recording sequence. When one wants to ensure stability throughout the image capturing sequence, it is virtually impossible to refocus the lens for optimal sharpness without disturbing it. The option of decreasing lens aperture (Nikon AF-D 60mm F/2.8 macro) to increase the depth of field proved, after testing, unsatisfactory with close-up imaging. The depth of field was also limited due to the use of the large 35mm sensor, compared to smaller sensor imagers that have a much bigger depth of field.

To counter the focus shift the CoastalOpt UV-VIS-IR 60mm Apo Macro lens (Jenoptik inc) was selected and acquired. Five of its 10 lens elements are made of calcium fluoride, enabling true apochromatic performance between 315 and 1100 nm.

Light Sources

LEDs were selected as light source. A total of 228 LEDs were evenly distributed across the inside of the Microdome. The white light Microdome was fitted with a high-powered neutral white LED, with a colour temperature of 4000° K. The MS Microdome was fitted with five different spectra. The selection of the bands was partly based on the spectra used within the Archimedes Palimpsest project (Archimedes Palimpsest 2010) and adopted towards the particularities of the PLD set-up. Since the PLD versions were planned in a way that most of their structure could be shared, the white light and multispectral LEDs required to have the same specifications such as size, construction, drive current, etc. They also had to be available in sufficient quantities. The choice fell on the LED Engin LZ1 product family. The five spectra selected are: UV 365 nm, Blue 465 nm, Green 523 nm, Red 623 nm and IR 850nm, each different types again evenly distributed across the dome. Their numbers vary from 44 to 48 LEDs per type. A simulation of different distribution patterns obtained through an even permutation of 5 different LEDs yielded the patterns in Fig. 25. The most even and symmetric distribution was selected and implemented (Fig. 26). The arrangement of the LEDs enabled the removal of a segment of the dome without sacrificing the overall distribution.

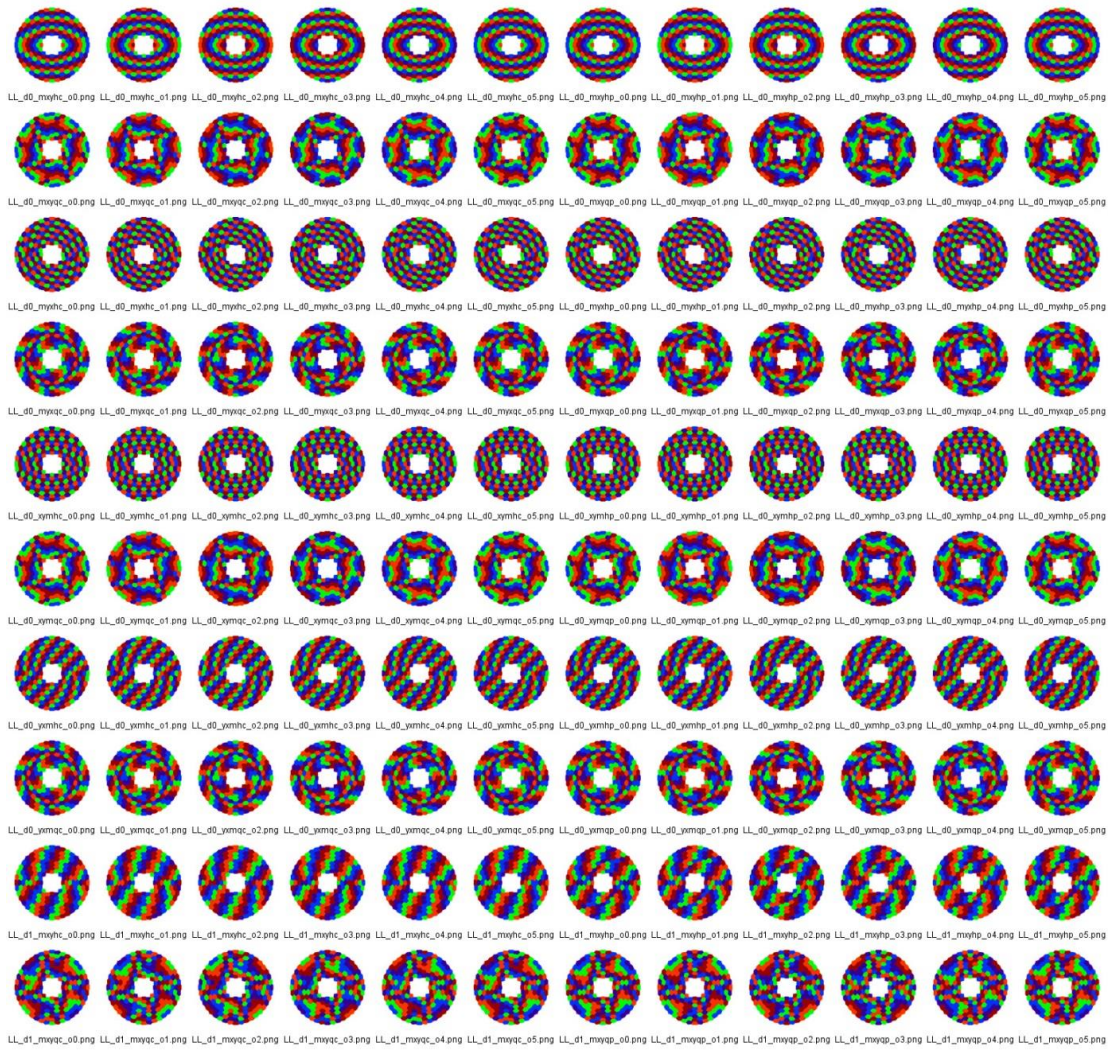


Figure 25: A choice of different permutations for the distribution of the 5 different LED emitters on the multispectral Microdome. (© RICH project & ESAT-VISICS, KU Leuven)

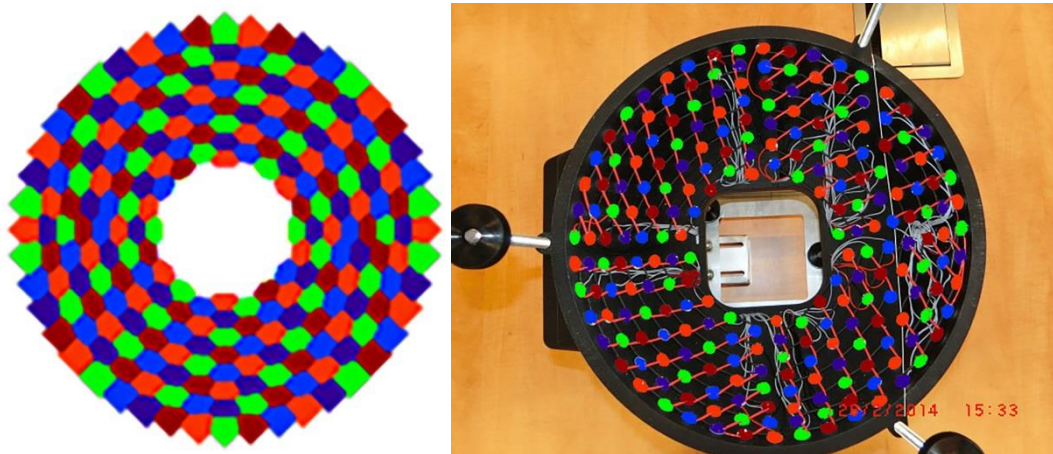


Figure 26: The selected distribution of the 5 different spectra implied on the inside of the Microdome. (© RICH project & ESAT-VISICS, KU Leuven)

2.2.3 The MS PLD Software

The results of the software package can be uploaded in a custom-made interactive (2D+) environment, the PLD viewer. The underlying methodology to determine the normal and surface information is based on the principles of Photometric Stereo (Woodham 1980; Horn 1986: Chapter 10-11; Verbiest and Van Gool 2008, Pevar et al. 2015). As opposed to Polynomial Texture Mapping (Malzbender et al. 2001; Earl et al. 2010), which tries to fit the observations with a mathematical function or description in order to mimic the appearance in a kind of make-believe visualisation, Photometric Stereo methods recover the actual 3D shape and albedo of a surface using multiple images in which the viewpoint is fixed and only the lighting directions vary. The technique is based on the fact that the amount of light reflected by a surface depends on the orientation of the surface in relation to the viewpoint of the camera and the position of the light source. The dome-shaped devices that we developed, consist of a single, down-looking camera on top of a hemisphere with LED light sources covering the inside surface. With this setup, the position of the object and the camera can be kept constant, while varying the position and angle of the light source by subsequently activating the different LEDs. Traditionally this method has only been verified with LED light sources of the same type, by default white light. Our starting point for the proposed algorithm is the existing CPU-only implementation (initiated in Willems et al. 2005; see also Watteuw et al. 2013).

The recovered results allow for both photorealistic and non-photorealistic virtual renderings of the scanned surfaces. To represent the geometry and the colour effectively, the currently implemented algorithm produces three output images: a normal image, an albedo image and an ambient image (Fig. 27). The normal image is a two-valued representation of the geometric details of the digitized object. It contains the surface orientation for each pixel and thus yields information on the overall physical shape of the object through integration of the pixel-wise normals.



Figure 27: The normal (left), albedo (center) and ambient (right) result images for the scan of a moth.
(© ESAT-VISICS, KU Leuven)

The albedo image contains the diffuse reflection coefficient for each pixel, providing information on the optical characteristics of the object's surface (Coakley 2003). The amount of energy that is reflected by a surface is determined by the reflectivity of that surface, called

the albedo. A high albedo means the surface reflects the majority of the radiation that hits it and absorbs the rest (Fig. 28).

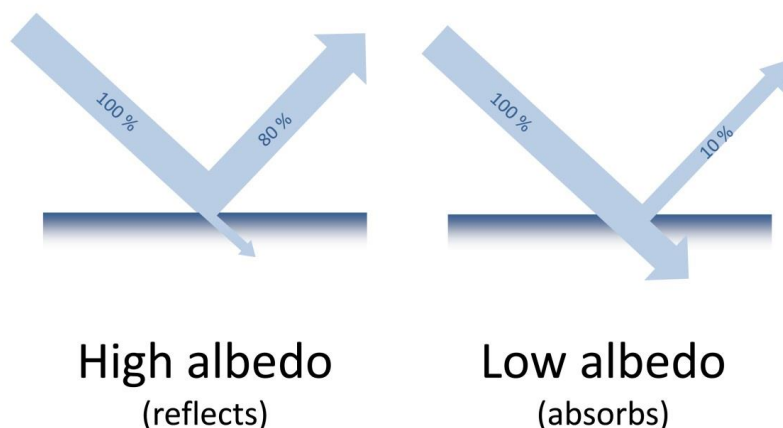


Figure 28: Example of the albedo principle (© KMKG-MRAH)

The interactive ambient image calculated by the software of the PLD viewer mimics the surface's observed colour when illuminated under ambient lighting conditions, in this particular case it simulates the effect of all the dome LEDs lighting that surface simultaneously. The albedo and normal map are used to create an accurate, textured 3D model of the digitized object. The ambient map serves as a comparison with (and alternative for) albedo, for inspection purposes for the users.

For the white light dome, the photometric stereo algorithm thus operates on a set of 260 images taken by the fixed camera – each with one LED activated – to produce the three output images, respectively containing the normal, the albedo and the ambient information for the observed object. For the multispectral dome, the algorithm is subdivided for the different types of LEDs available, i.e. a similar algorithm operates on the IR, R, G, B and UV components. Alternatively, the formulation of photometric stereo can be reformulated to keep the normal constant. It is, however, interesting to observe that the normal information that is extracted clearly tends to get crisper for shorter wavelengths (UV) and shows a gradual sharpening up from IR to UV. The physical phenomenon behind this is that electromagnetic energy at shorter wavelengths can detect smaller details (Fig. 29 & 30).

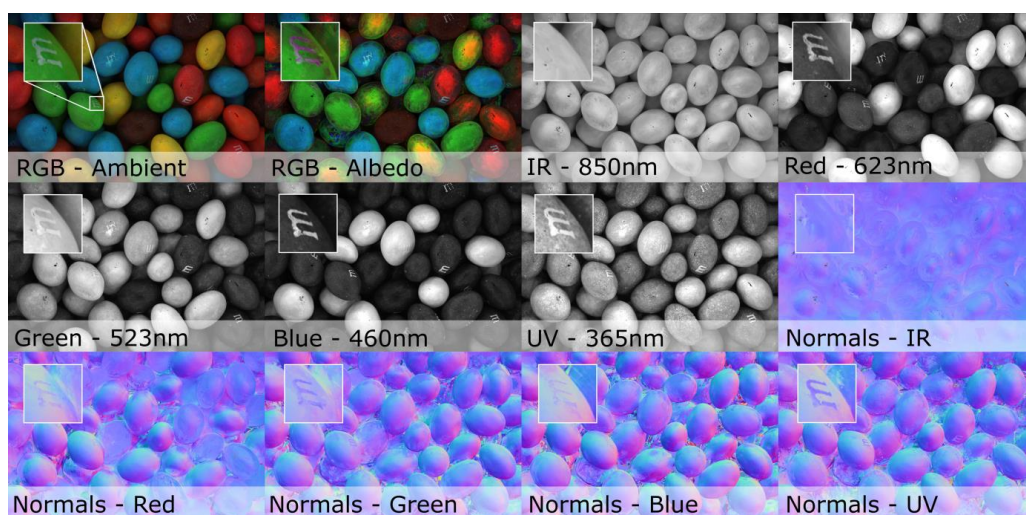


Figure 29: Overview of different visualisations of M&M's® by the PLD viewer software based on recordings by the MS Microdome, (© KMKG-MRAH & ESAT-VISICS, KU Leuven).

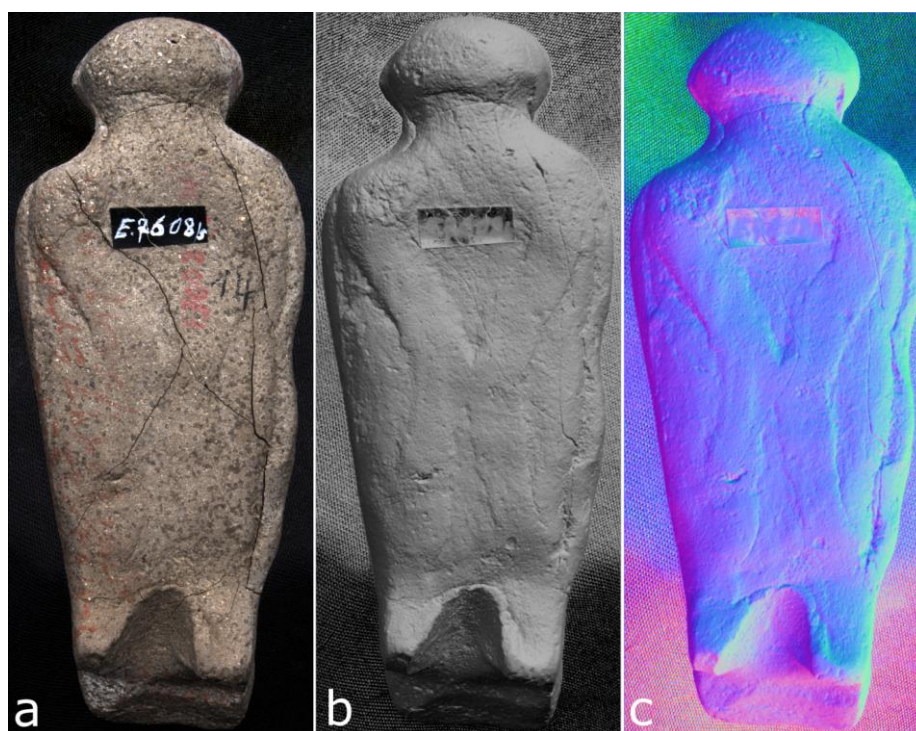


Figure 30: Verso of figurine E.7608. Interactive images produced by the PLD system. The different visualisations of the dataset reveal different aspects of the surface and the topography/relief: a) colour-sharpen filter; b) shaded filter; c) normal filter (© KMKG-MRAH; Portable Light Dome).

Reflection maps and histograms

In addition to false colour representations, the local reflectance on a surface can also be shown as a reflection map. For every pixel in the interactive PLD images the reflectance of that local surface structure is observed for each of the individual LED lights. The reflection map representing the layout of the interior of the dome shows the intensity of that reflectance. This observation can be computed for both the white light PLD and the MS PLD results. Obviously, exactly these observations are used by the software to determine the local surface normal, and

the corresponding reflectance characteristics. Thus, the reflection map can be used in its own right to investigate the nature of the local material properties.

The maps are observations or observed intensities (I) for a given pixel related to the angle between the incoming light (L) and the normal (N) at that position (Fig. 31). In its most fundamental form this relationship is given by the Bidirectional Reflectance Distribution Function (BRDF). In order to calculate the surface normal and material characteristics, most materials can be described by a lower dimensional parametric formulation. Photometric stereo has been introduced initially by assuming a Lambertian lighting model : $I = k_a \cdot L \cdot N$, where k_a is the albedo. In this context the principle has been extended using a Phong-like model that also allows including specular components. $I = k_a \cdot (L \cdot N) + k_s \cdot (R \cdot V)$, where k_s is a specular reflection constant, R the direction of the perfectly reflected ray and V the viewpoint of the observer.

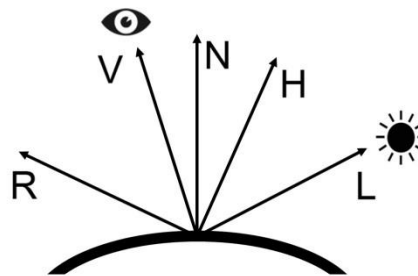


Figure 31: Model of observed reflections (© ESAT-VISICS, KU Leuven).

In Fig. 32 this approach is illustrated with a white light PLD recording explored further on in the paper. The reflectance of the metallic nature of the gold medallion is clearly shown by the specular peak it creates towards only those LEDs perpendicular to the inspected pixel (bright response), whereas the diffuse nature of the blue field (a more uniformly spread and dimmed brightness), demonstrates a close to perfect Lambertian response.

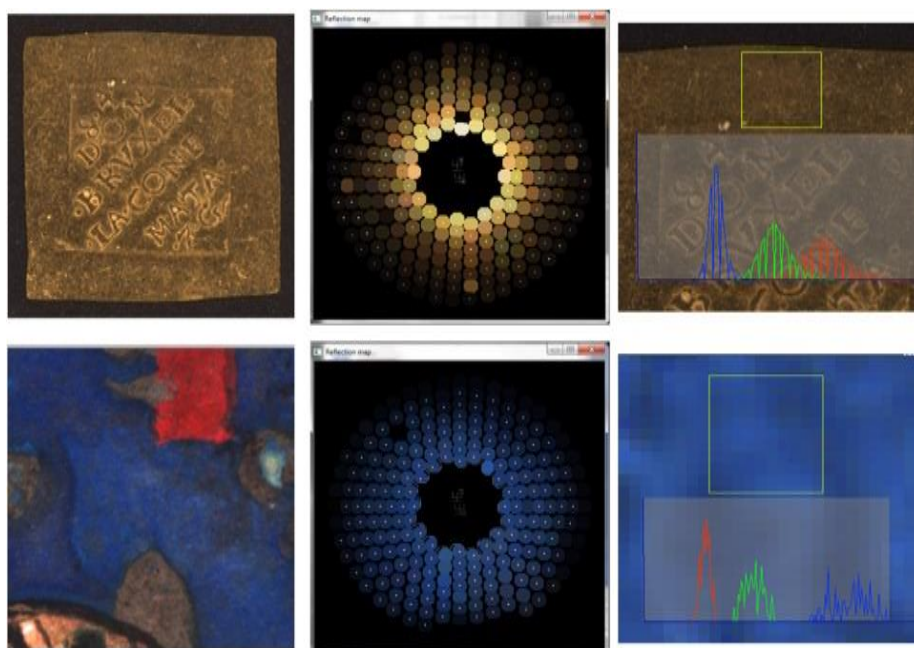


Figure 32: White light PLD reflection maps and histograms. Left: Golden medallion CBIB W827 (top) and detail of frontispiece Anjou Bible (bottom); Middle: reflection maps of one particular pixel; Right: histograms of a selected area (© RICH & ESAT-VISICS, KU Leuven).

For the MS PLD, the IR, R, G, B and UV channels are all displayed in one and the same map (Fig. 37-39, 41). In order to support the interpretation of the response, the local spectral content can also be presented within the PLD viewer interface as a histogram showing the distribution of calculated albedo responses for each of the spectral bands. In these histograms, the more the different bands are being plotted to the right, the higher their reflective response was for the selected area on the interactive PLD image (Fig. 37, 38, 40, 42). The albedo response is given by the x-axis, while the y-axis gives the probability distribution for each of the spectral components for the given area. As shown in Fig. 36 as well, for the white light dome this represents the distribution of RGB values of the extracted albedos in the given rectangular area. Typically, observations for a given material show a Gaussian distribution. The average response can be found where the distribution peaks.

2.2.4 The MS PLD Results

Enhancement of inscriptions

The MS imaging of the figurines is challenged by two types of inscriptions: iron-containing red ochre and carbon-containing black ink. Scientific studies dealing with MS imaging – predominantly on parchment, papyri and ostraca – describe that black (carbon) inks tend to give the best results in the IR spectrum, whereas visualizing remnants of red ochre inks are often very problematic. The results with the MS PLD system indicate the contrary. Even when only inspecting the general basic interactive images in the PLD viewer v6.01.03, entire new lines of the inscription in red ochre could be identified (Van der Perre et al. 2016, fig. 12). A Principal Component Analysis (PCA, see Fig. 33) based on these images demonstrates this excellent result distinctly. The black ink inscriptions on the other hand, gave only very poor responses,

especially in the IR spectrum where it is supposed to reach its best reflectance properties. This outcome aligns with new recent insights. Comparable research has shown the reflectance response of black carbon-containing pigments and clay is nearly the same in both VIS and IR spectral bands. As a consequence, neither in the VIS, nor in the IR sufficient contrast is reached to allow a differentiation between the zones with or without these pigment traces. When the pigment carrier is papyrus, paper or parchment, the reflectance response of both features is very similar in VIS, but sufficiently different in IR to reach a contrast that allows differentiation between pigments and background (Bearman and Christens-Barry 2009; Bearman et al. 2011).

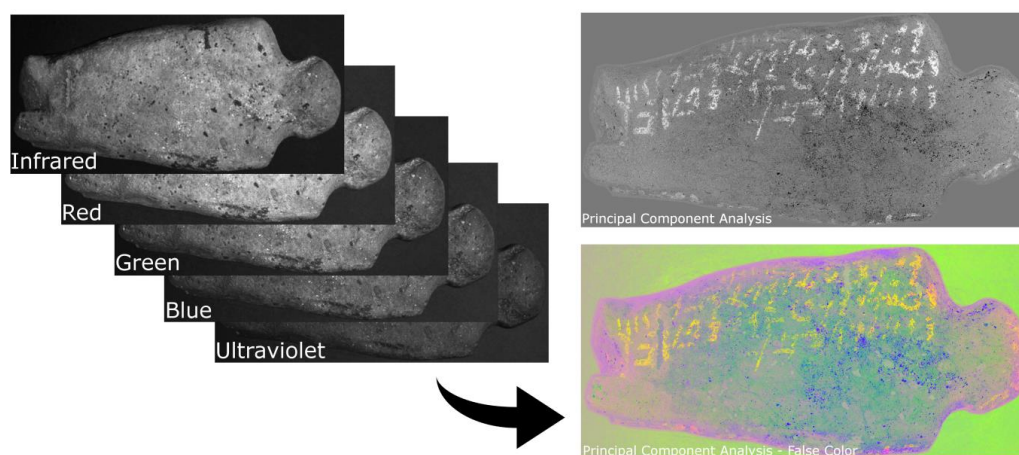


Figure 33: Verso of figurine E.9076 bearing red ochre inscription. Left: the recordings with the five different light spectra produced by the MS PLD system (© KMKG-MRAH; Portable Light Dome); Right: the PCA (Principal Component Analysis) calculations of this dataset (ImageJ software was used, courtesy of R.B. Toth Associates). The result reveals inscriptions no longer visible to the naked eye on the original.

The MS PLD can also enhance inscriptions by merely using the IR spectrum. An excellent example is the wooden headrest with Greek inscription, currently stored in the RMAH (Fig. 34). While the text is hardly readable with the bare eye due to a lack of contrast with the wooden surface, the IR image of the MS PLD immediately exposes all the lines of the inscription, even the faded passages in the centre.

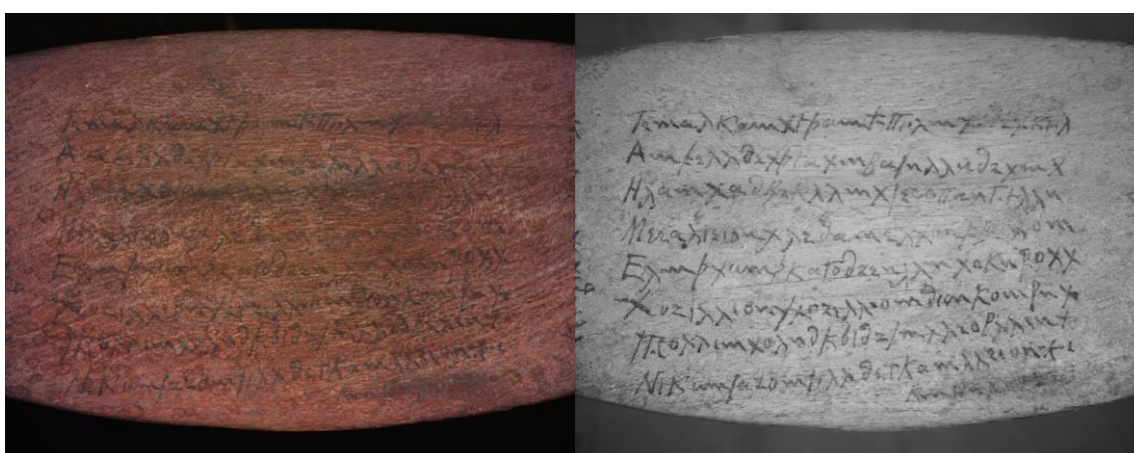


Figure 34: Ancient Egyptian headrest with Greek inscription. Left: MS PLD image in RGB, Right: MS PLD image in IR (© KMKG-MRAH)

Pigment and material study

The RICH and EES projects have been testing the system's potential for the study of pigments and materials. While it is clearly impossible to determine the chemical composition of a pigment solely based on the recordings of the MS dome, the system is actually capable to identify certain pigments and/or materials and therefore can be used as a preliminary, non-destructive research tool.

The following case studies present the value of the system for the identification of modern pigments and restorations, the distinction of gold and gold-like metals and the potential of the system for the study of blue pigments.

Case study 1: Modern pigments and restorations

One of the first possibilities encountered during these tests was the detection of modern pigments on ancient artefacts. Although they might appear similar in white light, it is common knowledge modern pigments used during the restoration of ancient objects will reflect light differently as the composition of their materials will differ from the original (ancient) materials. In the MS viewer interface of the PLD this can be visualised instantly by combining the five electromagnetic spectra of the MS PLD into false colour representations.

The heavily restored ancient Egyptian jar E.2458 (Fig. 35: A) at the RMAH proved to be an excellent case study to demonstrate this application. The modern pigments clearly react differently in the false colour images. In the presented case, the restored pieces are also recognisable with the naked eye and it therefore seems that the MS PLD images mainly confirm the expected result. However, they also show that the modern restoration paint overlaps the adjacent, original pigment (Fig. 35: B-C-D), providing important information for conservators. Similar results have been obtained on decorated objects where the restored parts cannot be discerned from the original with the naked eye (E.g. ancient Egyptian painted reliefs, statues and figurines). The MS PLD can thus be regarded as a valuable aid in conservation and restoration sciences, especially since the interactive consultation of these datasets, switching from one view mode to the other (e.g. Fig. 35: E-F), can be performed in real-time.

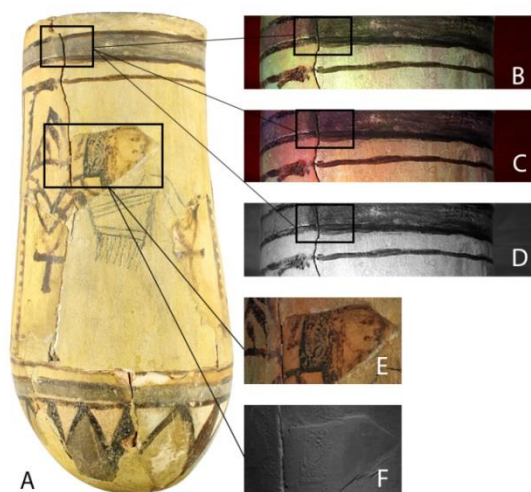


Figure 35: Ancient Egyptian decorated jar E.2458 (c. 1200 BCE): A) Conventional Digital photograph in white light; B) MS PLD false colour: IR/R/G; C) MS PLD false colour: IR/G/B; D) MS PLD: IR; E) MS PLD – R/G/B; F) MS PLD – shaded: surface characteristics (© KMG-MRAH).

Case study 2: Blue pigments in the Anjou Bible

During the study of the miniatures of the 14th century Anjou Bible in 2010 and 2016, highly detailed photographs with transmitted light in combination with non-destructive analysis and MS photometric stereo provided insights into the materials and techniques used by the medieval illuminator (e.g. Watteuw and Van Bos 2010: 147-170).

In the frontispiece of the Anjou Bible, king Robert of Anjou is depicted in front of a blue cloth with the Angevin coat of arms. The fleurs-de-lis are painted on top of a blue field, identified by μ -X-ray fluorescence (μ -XRF) measurements as being painted with azurite (rendering a large Cu peak in the XRF spectrum) (Watteuw and Van Bos 2010, 166, fol. 3v). During further examinations of the blue field, based on a MS PLD recording, a comparison of differently rendered false colour images revealed that the background must be composed of more than just one pigment; in the IR/G/B image a dark blue and a purple colour can be distinguished from each other (compare Fig. 36: B & C). In white light, however, this blue mixture used to paint the background has a very similar appearance (Fig. 36: A). As the XRF analyses could not identify with certainty the presence of another pigment, the most likely candidate for the (in white light blue appearing) material that becomes visible in the false colour image is ultramarine, made from lapis lazuli and not detectable by XRF. A definite identification of this pigment should always be confirmed by applying another technique (Trentelman 2012: 168, 178; Desnica et al. 2004: 15-21).

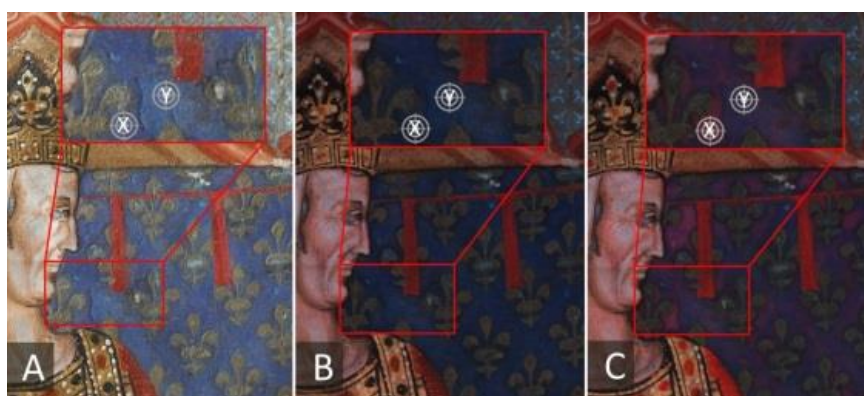


Figure 36: Detail frontispiece Anjou Bible: A) Conventional digital photograph in white light conditions; B) R/G/B image based on MS PLD dataset; C) False colour image, IR/G/B, based on MS PLD dataset; pigment in measure point Y has been identified as azurite by XRF (© RICH & ESAT-VISICS, KU Leuven).

The observations in the false colour rendering are also easily corroborated by the reflection maps and the local spectral statistics on the calculated albedo responses. Fig. 37 shows the reflection maps and histogram on an ultramarine and on an azurite painted area. When comparing both maps, it is easily observed there is a substantial difference in the IR responses. When taking a closer look at the local spectral distributions, one can observe the IR response for ultramarine is shifted towards the right (indicating a higher response), and in addition distinguish a smaller shift in UV, and ratio differences in R/G/B separately. Such observations made with this MS PLD system are supported by many similar spectral distribution analyses (Kartsonaki et al. 2007: 1-7, fig. 5-7; Delaney et al. 2005: 120-136).

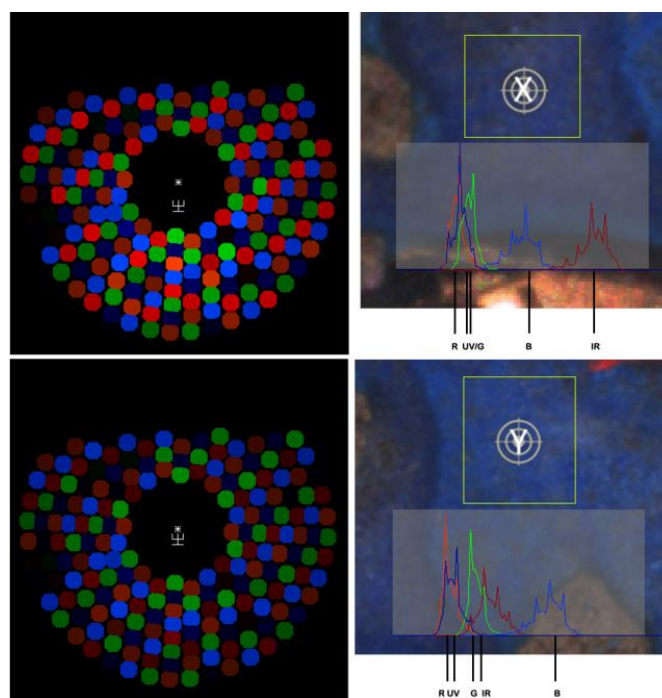


Figure 37: Reflection maps and histogram (screenshots from the MS PLD viewer v.7.0.02, R/G/B image in the back, both azurite and ultramarine appear as blue). Above: pixel and zone X (see Fig. 36), ultramarine; Below: pixel and zone Y (see Fig. 36), azurite (© ESAT-VISICS, KU Leuven)

In order to confirm the analysis, a MS PLD recording and analysis is carried out on the standard Pigments Checker v.2.1 by Cultural Heritage Science Open Source (CHSOS, <https://chsopensource.org>), containing a selection of 54 historical pigments. Again, the MS PLD reflection maps show a very similar behaviour (Fig. 38): besides both depicting an overall presence of blue, they show for the azurite ‘swatch’ on this Pigments Checker a higher reflectance in the green band (523 nm) and for the ultramarine ‘swatch’ a higher reflectance with the IR (850 nm) emitters. Interestingly, the ‘pure’ pigment swatches of the Pigment Checker reveal azurite has a very moderate response in IR and R with the MS PLD hardware; whereas the Bible of Anjou sample did give higher responses in IR (Fig. 38). This most probably indicates a certain degree of mixture of both the azurite and ultramarine pigments in the studied blue field. In conclusion, the reflectance information from the Anjou Bible and that of the Pigments Checker confirm the hypothesis that the blue field consists of two different materials and that their identification as azurite and ultramarine is most probable. In this case study, the MS PLD functioned as an aid in the identification of pigments that cannot be identified solely based on XRF datasets.

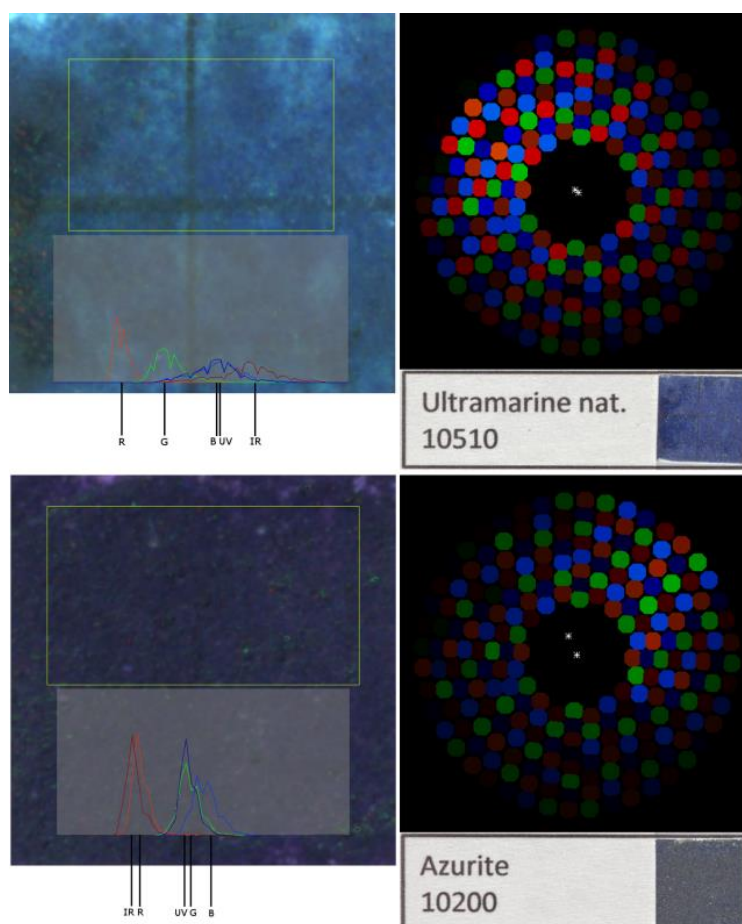


Figure 38: MS PLD reflection maps of the Pigments Checker (CHSOS); Above: ultramarine; Below: azurite (© RICH, KU Leuven)

Case study 3: Gold and metallic surfaces or paints

As a second case study, experiments have been set up to investigate the potentials of the PLD system to distinguish metallic surfaces or paints. Focus was laid in particular on the use of gold in medieval illuminations such as the Anjou Bible.

Even though it is obviously not possible to determine the karat rating or the percentage of other metals present in the alloy based on PLD images, the reflection maps of the white light and MS PLD nevertheless can assist in differentiating between gold and gold-like metals, which can be hard to distinguish with the naked eye. In order to gain insight in the matter, an experiment was set up using a set of 2 antique golden coins (CBIB O.I.613 and O.I.1), one inscribed golden medallion (CBIB W827), a modern 2 euro coin (Belgian) and a modern Egyptian 1 pound coin. The latter two have a 'golden look' but are made out of different alloys: for the 2 euro coin the inner segment consists of a gold coloured amalgam of 75% Cu, 20% Zn and 5% Ni (three layers: nickel brass, nickel, nickel brass), the Egyptian pound inner segment consists of an amalgam of 94% steel, 2% Ni and 4% Cu plating. All surfaces were recorded in one and the same acquisition session. The analysis is carried out on the extracted albedo values of the samples, to make sure the specular reflections do not influence the results. The false colour results and two reference reflection maps are shown in Fig. 39; histograms on four of the results in Fig. 40.



Figure 39: False colour representations and 2 examples of spectral reflectance responses on the collection of coins (MS PLD, © ESAT-VISICS, KU Leuven)

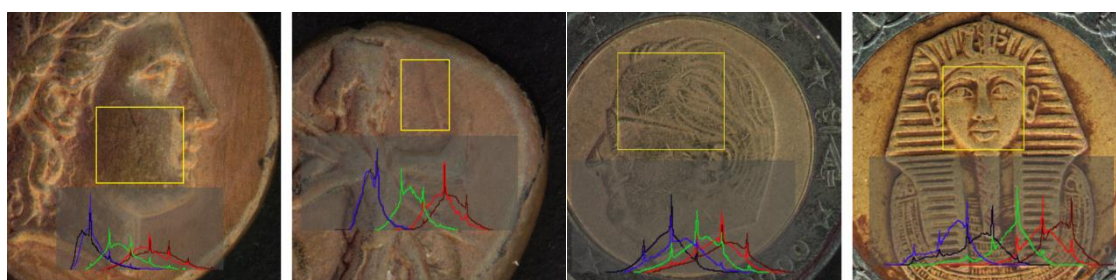


Figure 40: Reflectance histogram on the collection of coins (MS PLD, © ESAT-VISICS, KU Leuven)

For the gold surfaces similar reflection behaviour can be observed in the false colours, and the albedo of the euro coin is immediately isolated from all other results. The histograms give an even better insight. The genuine gold pieces show an almost perfect aligned UV and B spectral distribution; the R and IR curves show a very similar behaviour. The IR response reflectance for the Egyptian pound sample is even plotted completely to the right. Further, the relative ratios between the different bands renders the real gold pieces more 'greenish' than the (non-gold) modern coins. So again, the combination between the false colours, reflection maps and histograms gives sufficient indications to differentiate materials. When combined with known reference collections even particular materials can be identified.

Given these results, we used these observations to determine variations in gold coloured illuminating materials, in particular the difference in gold leaf and mosaic gold. In medieval illuminations, pure gold leaf and gold powder as a paint medium were already used in early Romanesque illumination. Another gold coloured layer in manuscripts is based on alloying a base metal (or metals) with a noble metal as described in the 14th century *De Arte Illuminandi* (Thompson and Hamilton 1933). According to this treatise, tin and/or lead were frequently alloyed with silver, whereas copper and silver were alloyed with gold. Tin sulphide (SnS₂) is described as an imitation gold. This so-called mosaic gold or *porporino* (Guineau 2005: 281) was able to replace costly 'true' gold, but it did not have the full brilliance of real gold.

The monitoring tools of the PLD system can, based on the various responses in the different spectral bands, distinguish real gold foil from mosaic gold. This is demonstrated with the bas-the-page miniature of the nativity on folio 230 verso, as shown in Fig. 41. XRF measurements of these layers in the Anjou Bible indicate that the two lions and the two colossus are painted in mosaic gold, whereas other elements, such as the background of the scene and the floral elements, are decorated with pure gold foil (Watteeuw and Van Bos 2010: 168, fol. 234, XRF n° 8 and XRF n° 23). In IR/R/G false colour mode, the real gold foil shows up as a darker greenish material (as was the case for the coins), an effect that is much lower in the areas with the mosaic gold. The specular peak is overall also higher for the foil than for the mosaic gold. As a comparison, the yellow bar in the shields below is not gold or metallic at all, but is painted in orpiment; thus, it shows a basically Lambertian behaviour. The spectral distribution on the lion and a piece of gold foil are presented respectively in Fig. 42. Here also, one can observe the difference in alignment in the UV and B channels, and the ratios between the other spectral bands that show similar patterns as were observed with the coin samples.



Figure 41: Bas-the-page miniature of the nativity on folio 230 verso of the Anjou Bible. Left: IR/R/G view, Right: R/G/B view, and reflectance maps. (MS PLD, © RICH & ESAT-VISICS, KU Leuven)



Figure 42: Spectral statistics on the lion painted in mosaic gold (left image) and the pure gold foil background (right image). (MS PLD, © RICH & ESAT-VISICS, KU Leuven)

Case study 4: Egyptian Blue and Visible-Induced Infrared Luminescence

In the above, applications of ‘normal’ multispectral reflectance methods have been discussed when combined with multi-light/directional reflectance techniques. The radiation of the incident light is known to what spectral band(s) it belongs and its interaction, the reflection of those particular band(s) only, with the surface is measured and used to create a (photorealistic) image or normal map. With the Portable Light Dome system one of the other MSI techniques has been pioneered as well: visible-induced infrared luminescence (VIL) imaging in combination with the multi-light/directional reflectance technique. With this technique the light emitted (so not reflected) by particular materials on the surface are used for imaging purposes. It acts in this study as an example and demonstration how many other MSI methods can be combined both with the principles of multi-light/directional reflectance imaging and with its existing acquisition approaches and devices.

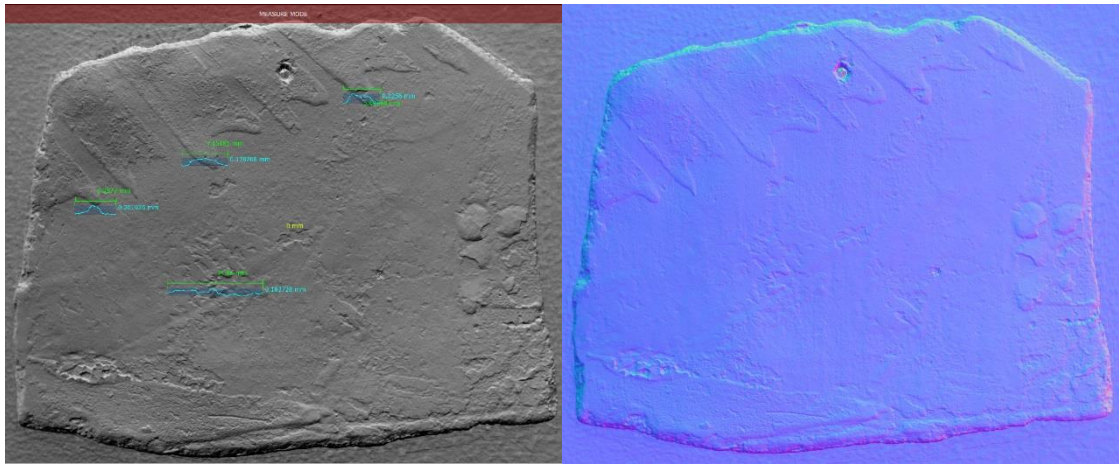
By understanding the reflective properties and qualities of certain materials (see also above) particular imaging strategies can be engineered to exploit them. In the case of the pigment Egyptian Blue these properties allow to isolate it in images when a correct acquisition setup has been followed. Egyptian Blue (Tite et al. 1987; Hatton et al. 2014) is one of the best known blue pigments applied and used in the ancient Near East and the Mediterranean (mid 3rd millennium up till the early Middle Ages). This inorganic, synthetic pigment is a cuprorivaite mineral ($\text{CaCuSi}_4\text{O}_{10}$ or calcium copper tetrasilicate). When visible light interacts with this cuprorivaite the luminescence wavelengths of the emitted light by this material consist of infrared radiation. The Cu^{2+} ions in this pigment are held responsible for this effect, a phenomenon known and described in literature as photo-induced luminescence; for early applications in heritage studies of Infrared Luminescence see Bridgman 1963; for Egyptian Blue, together with the pigments Han blue and Han purple, the effect has been studied extensively over the last two decades (Pozza et al. 2000), especially the work at the British Museum demonstrated the potential in polychrome art and for archaeological artefacts (Verri 2009a; Verri 2009b; Verri et al. 2010; Dyer, Verri & Cupitt 2013).

With visible-induced infrared luminescence – or photo-induced luminescence – when the Cu^{2+} ions in the Egyptian Blue are radiated with visual light they produce a very strong emission of wavelengths in the near infrared range (800-1700nm), any light sensor with sensitivity in this range can detect it; in fact, a sensitivity in 800-1000nm is sufficient (Verri 2009b). The excitation source in the visible range must be fluorescent lamps or LEDs, emitting close to no IR radiation; in most cases a benefit for this approach. The strongest emission by Egyptian blue has been measured in the 800-1100 nm range (Verri 2009b), centred at about 950nm (Verri 2009a). Therefore, in an acquisition setup when the ‘normal’ radiations – primarily in the visible range – are blocked by a longpass glass filter +800IR, only the emitted IR wavelengths above 800nm are registered. In the case-study we focus on, that will be a very strong emission (so high energy, appearing bright/white) by even the smallest remnants of Egyptian blue and only very little by all other pigments and materials on the surface which do not show this very strong luminescence effect (so non or low energy, appearing dark).

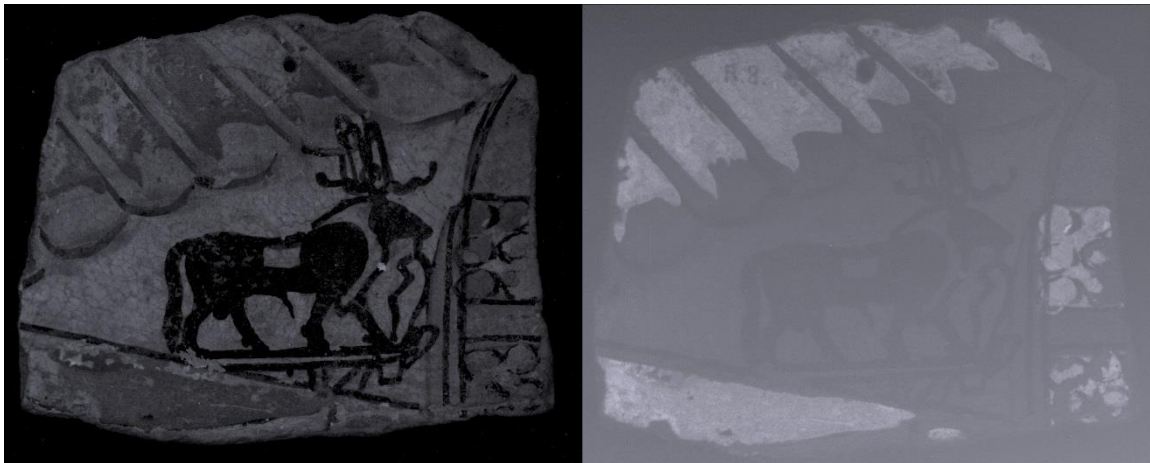
In Fig. 43 that principle is demonstrated with a small fragment of a polychrome New Kingdom cartonnage which was registered with the WL (so VIS) Portable Light Dome. The VIS LED's (CREE XLAMP 7090) in this WL PLD do not emit stray infrared radiation and can so perfectly serve this method. A glass longpass 830IR filter (Schott RG830) was installed in front of an Allied Vision Prosilica GT 6600 (OnSemi KAI29050 Mono) full spectrum (300-1000nm) light sensor mounted with the CoastalOpt 60mm UV-VIS-NIR lens. The comparison with a normal white light recording (image A) and the VIL result (image F) is evident. In the colour image several zones are clearly painted blue, most probably Egyptian blue. Images C-D illustrate the relief detected by the multi-light/directional reflectance technique when a recording is made with the 830IR longpass filter. It allows a study of the topography in detail, remark the Egyptian blue consist of a rather thick layer of pigment. By fixing the IR filter the luminescence effect becomes very visible. Image E is a recording with a longpass 715IR filter, as expected the effect is still minimal, compare with image B, the Egyptian blue highlight a little less dark. In image F the effect becomes very expressive. Most of the reflections by the incident visible light with the surface are blocked by the filter and only the IR wavelengths emitted by the Egyptian Blue are registered and appear as (bright) white. By including some of the multi-light/directional reflectance outcome, images G-H show only normal of the pixels in the areas with Egyptian Blue could be estimated, but as these are 'based' on the IR emissions of the pigment – not the reflection by the incident light- these cannot be used or trusted for geometrical studies.



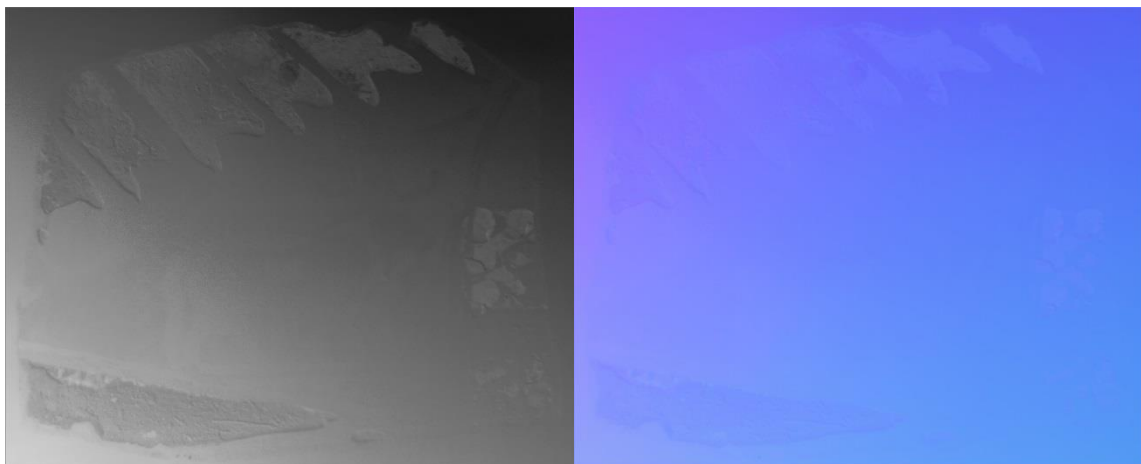
A) E.8802b: WL-dome, RGB-Manta camera, NO-filter, Colour/Sharpen image. B) E.8802b: MSI, WL-dome, Prosilica Full Spectrum camera, NO-filter, Texture/Sharpen image



C. E.8802b: MSI, WL-dome, Prosilica Full Spectrum camera, NO-filter, Shaded image with measurements. D. E.8802b: MSI, WL-dome, Prosilica Full Spectrum camera, NO-filter, Normal map



E. E.8802b: MSI, WL-dome, Prosilica Full Spectrum camera, VIL, IR715-filter, Texture image. F. E.8802b: MSI, WL-dome, Prosilica Full Spectrum camera, VIL, IR830-filter, Texture image



G. E.8802b: MSI, WL-dome, Prosilica Full Spectrum camera, VIL, IR830-filter, Shaded image. H. E.8802b: MSI, WL-dome, Prosilica Full Spectrum camera, VIL, IR830-filter, Normal map

Figure 43: Visible-induced infrared luminescence (VIL) of KMKG-MRAH E.8802b (all images are unprocessed images, direct results from PLDviewer 5.0.04b) (© KMKG-MRAH)

Remark on the example above also the area in the middle to the right. The VIL image (F) unmistakably shows a high response. Nevertheless, in the colour image (A) both blue, but especially a green substance is observed when visible light is applied. So the question must be raised whether the entire zone consists of the Egyptian blue pigment or not; the VIL images highlights the green areas white as well. An explanation might be found in a known degradation process Egyptian Blue can be affected by. It transforms the blue colour to a dark green or green-blue appearing substance (Scott 2010, 33). It is also observed Egyptian blue was mixed in antiquity with organic binding media. The Egyptian blue pigment itself remains stable, but that is not true for the organic binder in particular environmental conditions; it deteriorates. As a consequence, parts of the pigment fall off. In the case of E.8802b that phenomenon can be observed as well.

3. DISSEMINATION AND VALORISATION

3.1 Talks, Lectures & Workshops

- 1) 29 January 2015, Royal Belgian Institute of Natural Sciences (Brussels), “Seminar-at-Lunch-Time” meeting,
Anne Devillers and Vanessa Boschloos, *Antiquity@RMAH: Current Research*
- 2) 29 April 2015, KU Leuven - Digital Humanities Spring Session,
Bruno Vandermeulen, *New Adventures in Multispectral Imaging*.
<http://www.arts.kuleuven.be/digitalhumanities/DH-spring>
- 3) 5-6 May 2015, KU Leuven, Illuminare & Imaging Lab University Library, Multispectral Imaging Workshop, in collaboration with Lieve Watteeuw, Bruno Vandermeulen, Mike Toth, Barry Christens-Berry, Alberto Campagnolo, Eric Joakim, Marc Proesmans, Hendrik Hameeuw, Athena Van der Perre.
- 4) 22 July 2015, Porto, Lights On... Cultural Heritage and Museums!
Hendrik Hameeuw, Vanessa Boschloos, Luc Delvaux, Marc Proesmans, Bruno Vandermeulen, Athena Van der Perre, Luc Van Gool and Lieve Watteeuw, *The Combined Use of IR, UV and 3D Imaging for the Conservation and Study of Small Decorated and Inscribed Artefacts*
- 5) 25 August 2015, Florence, International Congress of Egyptologists XI
Athena Van der Perre, *The Egyptian Execration Statuettes (EES) Project*
- 6) 4 October 2015, RMAH Brussels, International Conference Archaeometallurgy: Non-Ferrous Metals Metallurgy and Experimental Archaeology,
Hendrik Hameeuw, *Registration and Safeguarding data in the Field and in the Museum, Some Strategies*.
- 7) 24 October 2015, The Hague, 43e Nederlands-Vlaamse Egyptologendag,
Athena Van der Perre, *Multispectrale 3D-beeldvorming in de KMKG: Het EES project*
- 8) 4-6 November 2015, Leipzig, Digital Humanities in Egyptology,
Athena Van der Perre, *From Execration Texts to Quarry Inscriptions: Combining IR, UV and 3D-Imaging for the Documentation of Hieratic Inscriptions*.

- 9) 18 November 2015, RMAH Brussels, Persdag
Hendrik Hameeuw and Athena Van der Perre, Nieuwe Beeldvormingstechnieken voor het erfgoed van het Midden-Oosten
- 10) 27 November 2015, Brussels, Towards DARIAH-BE: a kick-off meeting with the launch of the Digital Humanities Research Community Flanders,
Hendrik Hameeuw and Chris Vastenhoud, Digital Humanities in a scientific museum context: the case of KMKG-MRAH.
- 11) 13 January 2016, Hebrew University of Jerusalem,
Hendrik Hameeuw, Light on artefacts: What the Portable Light Dome system can do for ancient Near Eastern Archaeology.
- 12) 6 March 2016, RMAH Brussels, Lezing Educatieve Dienst
Athena Van der Perre, Vervloekt! Verwensingsrituelen in het Oude Egypte
- 13) 16 March 2016, RBINS Brussels, International conference Non-destructive and Destructive Methods to Identify Archaeological Finds and their Host Deposits in Arid and Semi-arid Areas
Hendrik Hameeuw and Athena Van der Perre, The Use of Multispectral Visualizations for the Identification of Pigment Patterns
- 14) 21-25 March 2016, Ghent, 2nd International Conference on Innovation in Art Research and Technology (InArt), Flash Poster Session (1-1-1)
Lieve Watteeuw, Hendrik Hameeuw, Bruno Vandermeulen, Athena Van der Perre, Vanessa Boschloos, Luc Delvaux, Marc Proesmans, Marina van Bos and Luc Van Gool, Light, Shadows and Surface Characteristics. The Multispectral Portable Light Dome
- 15) 24 November 2016, San Antonio (Texas), ASOR Annual Meeting, ASOR TV
Vanessa Boschloos, New Lights on the Brussels Egyptian Execration Figurines (see <https://youtu.be/Ki8TKHZ6jSo>)
- 16) 2 February 2017, Heidelberg University - Materiale Textkulturen - Teilprojekt A03
Athena Van der Perre, Putting the Egyptian Execration Figurines Back in the Limelight
- 17) 28 February 2017, KU Leuven, Egyptologica Vlaanderen
Athena Van der Perre, Vervloekte Figurines! De geheimen van de Egyptische verwensingsbeeldjes ontsluit
- 18) 2 March 2017, Ghent University, Egyptologica Vlaanderen
Athena Van der Perre, Vervloekte Figurines! De geheimen van de Egyptische verwensingsbeeldjes ontsluit
- 19) 7 March 2017, RMAH Brussels, Science@Lunch
Hendrik Hameeuw and Athena Van der Perre, "I see wonderful things". Ontwikkeling en gebruik van een nieuw multispectraal systeem voor beeldmateriaal: MS PLD (Portable Light Dome).

3.2 Posters

- Watteeuw Lieve, Hameeuw Hendrik, Vandermeulen Bruno, Van der Perre Athena, Boschloos Vanessa, Delvaux Luc, Proesmans Marc, Van Bos Marina and Luc Van Gool (2016), Light, Shadows and Surface Characteristics: The Multispectral Portable Light Dome, InArt 2016, Ghent, March 2016
[https://www.academia.edu/23689313/Light_Shadows_and_Surface_Characteristics_The_Multispectral_Portable_Light_Dome]
- Boschloos Vanessa, Hameeuw Hendrik and Athena Van der Perre, New Lights on the Brussels Execration Figurines, ASOR meeting 2016, San Antonio, Texas, November 2016. (DOI: 10.13140/RG.2.2.25330.91841)
[https://www.researchgate.net/publication/310793561_NEW_LIGHTS_ON_THE_BRUSSELS_EGYPTIAN_EXECRATION_FIGURINES_1_Dealing_with_conservation_issues]

3.3 Websites & Blogs

- EES page on RMAH website : <http://www.kmkg-mrah.be/conservation-ir-uv-and-3d-imaging-egyptian-execration-statuettes-ees-project>
- Portable Light Dome blog : <https://portablelightdome.wordpress.com/>
 - Hameeuw, H., Van der Perre, A., 2015. First preliminary results of the Egyptian Execration Statuettes (EES) Project. <https://portablelightdome.wordpress.com/2015/05/06/first-preliminary-results-of-the-egyptian-execration-statuettes-ees-project/>
- Youtube videos:
 - Portable Light Dome System: Multispectral Microdome. Imaging an Egyptian mummy portrait at the Royal Museums of Art and History – Brussels: <https://youtu.be/Gz7DmamlETk>
 - New Lights on the Brussels Egyptian Execration Figurines: <https://youtu.be/Ki8TKHZ6jSo>

4. PERSPECTIVES

- The EES project has demonstrated the overwhelming potential of the MS Portable Light Dome system for the visual documentation, study and virtual safeguarding of a large number of various types of cultural heritage artefacts. As a scientific institute, this **new research infrastructure** gives the Royal Museums of Art and History and its partners at the KU Leuven a head start in their future activities.
- The abilities of the analytic tools incorporated in the MS PLD software to characterize materials and pigments based on their reflective properties and the promising set of extensions towards additional MSI techniques in combination with multi-light/directional reflectance techniques (see 2.2.4, case study 4) are in fact only merely in their infancy. Their **potential for heritage and conservation studies** is

extensive. Future projects and tests must be conducted to further explore the uses of this innovative approach.

- The project has emphasised the major historical importance of the Saqqara execration figurines, being **Prime Cultural Heritage Artefacts**. By making this exceptional collection the case-study of a pioneering research project, the RMAH strives to give a renewed boost to the study of these objects. The condition assessment presented valuable insights for the future conservation and preservation of these artefacts.
- Revisiting the collection more particularly underscored the necessity of advancing in their study given their state of preservation, especially since valuable information is inevitably lost. In spite of their current condition, the observations also demonstrate that, even though the figurines have been amply discussed in the literature, previous scholarship focussed mainly on the texts of the large figurines, and a wealth of information subsequently remains to be explored (e.g. regarding technological aspects, typological questions and epigraphy). The EES project has proven that the combined effort of setting up an extended **conservation management** plan and developing the MS PLD, makes it possible to document the figurines' surfaces in detail and bring out faded inscriptions, thus making revising the existing translations and translating the unpublished inscriptions feasible again. Despite the historical importance of these figurines, they are currently threatened by several causes, not in the least by their own fragility. One of the recommended actions is to improve the storage of these figurines, but the most urgent action is to consolidate the figurines currently categorised as Conservation Category 4. In a second phase, those in Categories 2 and 3 must be treated. Immediate action and investment must take place!
- Apart from the restoration or consolidation of the figurines, an important task of the conservation work lies in documenting these objects. To some extent this has already been realised by the EES Project, where a selection of the collection is already documented with a prototype of the MS PLD, the MS Microdome. The prototype is of slightly smaller dimensions than the dome device that will be available for documenting the remaining figurines. The final objective is to have the **entire collection** of execration figurines **documented** for analysis with this MS PLD, and, in a next phase, to make these recordings accessible for the scientific community. Consequently, this will allow scholars all over the world to study this exceptional collection of artefacts without the need to handle the fragile objects.

5. PUBLICATIONS

Van der Perre Athena and Hendrik Hameeuw (2015), La création d'images multi-spectrales: les portraits romains du Fayoum, in: Luc Delvaux and Isabelle Therasse (eds.), *Sarcophages. Sous les étoiles de Nout*, Brussels, 164-165.

[https://www.academia.edu/17039454/La_cr%C3%A9ation_dimages_multi-spectrales_les_portraits_romains_du_Fayoum_in_Delvaux_L_et_I_Therasse_Sarcophages._Sous_les_%C3%A9toiles_de_Nout_2015_164-165]

Van der Perre Athena and Hendrik Hameeuw (2015), Multispectrale Beeldvorming: de Romeinse mummieportretten van de Fajoem, in: Luc Delvaux and Isabelle Therasse (Eds.). *Sarcofagen: Onder de sterren van Noet*, Tielt, 164-165.

[https://www.academia.edu/17039605/Multispectrale_beeldvorming_de_Romeinse_mummieportretten_van_de_Fajoem_in_L_Delvaux_en_I_Therasse_Sarcofagen._Onder_de_sterren_van_Noet_2015_164-165]

Van der Perre Athena (2016), From Execration Texts to Quarry Inscriptions: Combining IR, UV and 3D Imaging for the Documentation of Hieratic Inscriptions, in: Monica Berti and Franziska Naether (eds.), *Alturtumswissenschaften in a Digital Age: Egyptology, Papyrology and beyond; Proceedings of a conference and workshop in Leipzig, November 4-6, 2015*, Leipzig.

[[http://www.qucosa.de/recherche/frontdoor/?tx_slubopus4frontend\[id\]=20190](http://www.qucosa.de/recherche/frontdoor/?tx_slubopus4frontend[id]=20190)]

Watteeuw Lieve, Hameeuw Hendrik, Vandermeulen Bruno, Van der Perre Athena, Boschloos Vanessa, Delvaux Luc, Proesmans Marc, Van Bos Marina and Luc Van Gool (2016), Light, Shadows and Surface Characteristics. The Multispectral Portable Light Dome, *Applied Physics A* 122: 976, 1-7.

[https://www.researchgate.net/publication/309567127_Light_shadows_and_surface_characteristics_the_multispectral_Portable_Light_Dome, peer reviewed,, IF: 1.444]

Van der Perre Athena, Hameeuw Hendrik and Vanessa Boschloos (2016), The Multispectral Portable Light Dome: Documenting the Egyptian Execration Figurines of the Royal Museums of Art and History, Brussels, *Journal of Ancient Egyptian Interconnections* 11, 21-22.

[https://www.researchgate.net/publication/311173525_The_Multispectral_Portable_Light_Dome_Documenting_the_Egyptian_Execration_Figurines_of_the_Royal_Museums_of_Art_and_History_Brussels]

Van der Perre Athena, Hameeuw Hendrik, Boschloos Vanessa, Delvaux Luc, Proesmans Marc, Vandermeulen Bruno, Van Gool Luc and Lieve Watteeuw (2016), Towards a combined use of IR, UV and 3D-imaging for the study of small inscribed and illuminated artefacts, in Paula Menino Homem (ed.), *Lights On... Cultural Heritage and Museums!*, Porto, 163-192.

[https://www.academia.edu/30700589/Towards_a_combined_use_of_IR_UV_and_3D-Imaging_for_the_study_of_small_inscribed_and_illuminated_artefacts, peer reviewed]

Van der Perre Athena, The Egyptian Execration Statuettes Project, in: *Proceedings of the International Conference of Egyptologists XI, Florence, 2015* (in press).

Van der Perre Athena, Braekmans Dennis, Boschloos Vanessa, Ossieur France, Hameeuw Hendrik and Luc Delvaux, The Egyptian Execration Figurines of the Royal Museums of Art and History, Brussels: Conservation, Pigments and Digitisation, in *Bulletin des Musées royaux d'Art et d'Histoire, Bruxelles* 85 (2014) (in press).

Braekmans Dennis, Boschloos Vanessa, Hameeuw Hendrik and Athena Van der Perre, Tracing Unfired Ancient Egyptian Execration Figurines Through Non-Destructive X-Ray Spectrometry Analysis (forthcoming).

6. ACKNOWLEDGEMENTS

As authors we are particularly grateful to dr. Eric Gubel, Senior Keeper of the Antiquity Department at the RMAH, who drew our attention to this fascinating group of execration figurines and the urge to document and reassess them. We like to thank dr. Luc Limme for his valuable suggestions, and Monique Deruette and Martine Gruselle for their help in the archives of the museum and the Fondation Égyptologique. Thanks are also due to the museum's photographer Raoul Pessemier for providing additional colour illustrations.

The colleagues at the KU Leuven with whom we have collaborated in the development of the MS PLD system are also thanked: dr. Marc Proesmans, Bruno Vandermeulen and dr. Lieve Watteeuw. We are furthermore grateful to dr. Stan Hendrickx (Hasselt, MAD-Faculty) for his observations regarding the clay composition of the figurines, and to dr. Elena Marinova (Center for Archaeological Sciences (KU Leuven) and Royal Belgian Institute of Natural Sciences of Brussels) for the identification of botanical remains. We also like to thank the Griffith Institute (Oxford) for providing access to the personal archives of Gunn and Cerny.

Finally, we warmly thank dr. Marina Van Bos and dr. Steven Saverwyns for the Large Area Micro XRF and Micro-Raman Spectroscopy analyses at the KIK-IRPA Brussels. And we thank dr. Peter Vandenaabeele and Sylvia Lycke for the Raman mapping at the Raman Spectroscopy Research Group (Ghent University).

Special thanks go to the people involved in the Portable Light Dome projects and development:

Anne Goddeeris, Bert Deknuydt, Elena Devecchi, Anne Devillers, Stefan Gradmann, Elynn Gorris, Jared Miller, Wim Moreau, Bruno Overlaet, David Owen, Stéphane Polis, David Tingdahl, Fred Truyen, Jan Van der Stock, Luc Van Gool, Karel Van Lerberghe, Sam Van Overmeire, Vincent Vanweddingen, Frank Verbiest, Gabriella Voet, Lieve Watteeuw, Geert Willems.

7. REFERENCES

Abate, F., Menna, F, Remondino, F. and M.G. Gattari (2014), '3D painting documentation: evaluation of conservation conditions with 3D imaging and ranging techniques', *The International Archives of the Photogrammetry, Remote Sensing and Spatial Information Sciences XL-5(V/WG2)*, 1–8.

Abdalla, A. (1992), 'The Cenotaph of the Sekwaskhet Family', *Journal of Egyptian Archaeology* 78, 93-111.

Archimedes Palimpsest (2010), core Archimedes data [online]. Available from: <http://archimedespalimpsest.net/Data/> [Accessed 23th November 2015] .

Arnold, D. and J. Bourriau (1993), *An Introduction to Ancient Egyptian Pottery*, DAIK Sonderschriften 17, Mainz am Rhein.

Bay, S., Bearman, G., Macfarlane, R. and T. Wayment (2010), 'Multi-Spectral Imaging vs Monospectral Infrared Imaging', *Zeitschrift fur Papyrologie und Epigraphik* 173, 211-217.

Bearman, G.H, Anderson, M.S. and K. Aitchison (2011), 'New Imaging Methods to Improve Text Legibility of Ostraca', *PalArch's Journal of Archaeology of Egypt/ Egyptology* 8/2, 1-7.

Bearman, G.H. and W.A. Christens-Barry (2009), 'Spectral Imaging of Ostraca', *PalArch's Journal of Archaeology of Egypt/Egyptology* 6/7, 1-20.

Bennett, T. (2015), 'Photogrammetry and Transmitted Infrared Imaging to Document the Support of a 19th c. British Landscape Painting', *COSCH e-Bulletin* 2, 1-10.

Ben-Tor, A. (2006), 'Do the Execration Texts reflect an accurate picture of the contemporary settlement map of Palestine?', in: Y. Amit et al. (eds.), *Essays on Ancient Israel in Its Near Eastern Context: A Tribute to Nadav Na'aman*, Winona Lake, 63-87.

Bierbrier, M.L. (2012), *Who Was Who in Egyptology*⁴, London.

Blom-Boër, I. (1994), 'Zusammensetzung altägyptischer Farbpigmente und ihre Herkunftslagerstätten in Zeit und Raum', *Oudheidkundige Mededelingen uit het Rijksmuseum van Oudheden te Leiden* 74, 55-107.

Boon, J. and E. Leonardt (2015), 'New Light on the Surface of Art Objects in the Conservation Studio with a 3D Digital Hirox Microscope Mounted on an XYZ Stand', in: *Practical Philosophy, or Making Conservation Work. Abstract book AIC 43rd Annual Meeting, May 13-16 2015*, Miami. Available from: <http://www.conservation->

us.org/docs/default-source/annualmeeting/2015am_poster_8.pdf [Accessed 19th November 2015].

Booras, S.W. and D.R. Seely (1999), 'Multispectral Imaging of the Herculaneum Papyri', *Cronache Ercolanesi* 29, 95-100.

Bourriau, J., Nicholson, P. & P. Rose (2000), 'Pottery', in: Nicholson, P. & I. Shaw (eds.), *Ancient Egyptian Materials and Technology*, Cambridge, 121-147.

Braekmans, D., Boschloos, V., Hameeuw, H. and A. Van der Perre (forthcoming), 'Tracing Unfired Ancient Egyptian Execration Figurines Through Non-Destructive X-Ray Spectrometry Analysis'.

Bridgman C.F. (1963), 'Infrared Luminescence in the Photographic Examination of Paintings and Other Art Objects', *Studies in Conservation* 8, 77-83.

Bülow-Jacobsen, A. (2008), 'Infra-red imaging of ostraca and papyri', *Zeitschrift für Papyrologie und Epigraphik* 165, 175-185.

Caine, M. and M. Magen (2011), 'Pixels and Parchment: The Application of RTI and Infrared Imaging to the Dead Sea Scrolls', in: Dunn, S., Bowen, J. and K. Ng (eds.), *EVA London 2011: Electronic Visualisation & the Arts. Proceedings of a conference held in London 6-8 July*, Swindon, 140-146.

Capart, J. and G. Posener (1939), 'Figurines égyptiennes d'envoûtement', *Comptes Rendus des séances de l'Académie des Inscriptions et Belles-Lettres* 83(1), 66-74.

Casaletto M.P., Ingo G.M., Riccucci C., de Caro T., Bultrini G., Fragalà I. and M. Leoni (2008), 'Chemical cleaning of encrustations on archaeological ceramic artefacts found in different Italian sites', *Applied Physics A* 92(1), 35-42

Coakley, J.A. (2003), 'Reflectance and Albedo, Surface', in: Holton, J.R. and J.A. Curry (eds.), *Encyclopedia of the Atmosphere*, Corvallis, 1914-1923.

Corcoran, L.H. and M. Svoboda (2010), *Herakleides. A portrait mummy from Roman Egypt*, Los Angeles.

Cosentino, A. (2014), 'Identification of pigments by multispectral imaging; a flowchart method', *Heritage Science* 2(8), 1-12.

Delaney, J.K., Walmsley, E., Berrie, B.H. and C. F. Fletcher (2005), 'Multispectral Imaging of Paintings in the Infrared to Detect and Map Blue Pigments', in: *Scientific Examination of Art – Modern Techniques In Conservation and Analysis*, Washington D.C., 120-136

Desnica, V., Furic, K. and M. Schreiner (2004), 'Multianalytical Characterization of a variety of Ultramarine pigments', *e-PS* 2004 (1), 15-21.

Dyer, J., Ambers, J. and A. Simpson (2012), Analysis of pigment traces on a limestone sculpture of the Egyptian god Horus in Roman military costume (1912,0608.109). British Museum (unpublished). Available from: http://www.britishmuseum.org/pdf/AR2012_42_Horus%20in%20Roman%20military%20costume.pdf [Accessed 9th November 2015].

Dyer J., Verri G. and J. Cupit (2013), 'Multispectral Imaging in Reflectance and Photo-induced Luminescence modes: A User Manual', London.

Earl, G., Martinez, K. and T. Malzbender (2010), 'Archaeological applications of polynomial texture mapping: analysis , conservation and representation', *Journal of Archaeological Science* 37, 1-11.

Easton, R.L. Jr., Christens-Barry, W.A. and K.T. Knox (2011), 'Ten Years of Lessons from Imaging of the Archimedes Palimpsest', in: Vahtikari, V., Hakkarainen, M. and A. Nurminen (eds.), *Eikonopoiia: digital imaging of ancient textual heritage*, Helsinki, 5-33.

Faigenbaum, S., Sober, B., Shaus, A., Moinester, M., Piasetzky, E., Bearman, G., Cordonsky, M. and I. Finkelstein (2012), 'Multispectral images of ostraca: acquisition and analysis', *Journal of Archaeological Science* 39(12), 3581-3590.

Firth, C.M. and B. Gunn (1926), *Teti Pyramid Cemeteries*, Excavations at Saqqara, Cairo.

Ganio, M., Salvant, J., Williams, J., Lee, L., Cossairt, O. and M. Walton (2015), 'Investigating the use of Egyptian blue in Roman Egyptian portraits and panels from Tebtunis, Egypt', *Applied Physics A* 121(3), 813-821.

Guineau, B. (2005), *Glossaires des matériaux de la couleur et des termes techniques employés dans les recettes de couleurs anciennes*, *De diversis artibus* 73, Turnhout.

Hameeuw, H. and G. Willems (2011), 'New Visualization Techniques for Cuneiform Texts and Sealings', *Akkadica* 132, 163-178.

Hatton G.D., Shortland A.J. and M.S. Tite (2014), 'The production technology of Egyptian blue and green frits from the second millennium BC Egypt and Mesopotamia', *Journal of Archaeological Science* 35, 1591-92. DOI:10.1016/j.jas.2007.11.008

Horn, B.K.P. (1986), *Robot Vision*, Cambridge.

Kartsonaki, M., Kouli, M., Callet, P. and E. Cheilakou (2007), 'Non-destructive identification of the colouring substances on the monuments', in: *Proceedings of the 4th international conference on (NDT)*, Chania, 1-7.

Keats Webb, E. (2015), '3D and near-infrared imaging for object documentation', SEAHA [Poster]. Available from: <https://www.bartlett.ucl.ac.uk/heritage/programmes/mres-msc/mres-seaha/images/keatsposter2015> [Accessed 18th November 2015].

Kotoula E. (2012), 'Infrared RTI: Experimentation towards the development of multispectral RTI', *Archaeology Blogs Southampton University* [online]. Available from: <http://acrg.soton.ac.uk/blog/1569/> [Accessed 25th November 2015].

Kotoula, E. (2015), 'Ultraviolet RTI', *Archaeology Blogs Southampton University* [online]. Available from: <http://acrg.soton.ac.uk/blog/4175/> [Accessed 9th November 2015].

Lee, L. and S. Quirke (2000), 'Painting Materials' in: P. Nicholson and I. Shaw (eds.), *Ancient Egyptian Materials and Technology*, Cambridge, 104-120.

Macfarlane, R.T., Wayment, T., Bay, S.M. and G. Bearman (2011), 'Exploring the Limitations and Advantages of Multi-Spectral Imaging in Papyrology: darkened, carbonized, and palimpsest papyri', in: Vahtikari, V., Hakkarainen, M. and A. Nurminen (eds.), *Eikonopoiia: digital imaging of ancient textual heritage*, Helsinki, 87-98.

Malzbender, T., Gelb, D. and H. Wolters (2001), Polynomial texture maps, in: *SIGGRAPH'01: Proceedings of the 28th Annual Conference on Computer Graphics and Interactive Techniques, 12-17 August 2001*, New York, 519-528.

O'Grady, C. (2005), 'Morphological and chemical analyses of manganese dioxide accretions on mexican ceramics', in: P. Vandiver et al. (eds.), *Materials issues in art and archaeology*, vol. 7. Materials Research Society Symposium Proceedings 852, Pittsburgh, 183-192.

Pevar, A., Verswyvel, L., Georgoulis, S., Cornelis, N., Proesmans, M. and L. Van Gool (2015), 'Real-time Photometric Stereo', in: D. Fritsch (ed.), *Photogrammetric Week '15*, Stuttgart, 185-206.

Pinch, G. (2001), 'Red Things: the symbolism of colour in magic', in: W.V. Davies (ed.), *Colour and Painting in Ancient Egypt*, London, 182-185.

Posener, G. (1939), 'Nouvelles listes de proscription (Ächtungstexte) datant du Moyen Empire', *Chronique d'Égypte* 27, 39-46.

Posener, G. (1940), *Princes et pays d'Asie et de Nubie. Textes hiéroglyphiques sur des figurines d'envoûtement du Moyen Empire*, Bruxelles.

Posener, G. (1987), *Cinq figurines d'envoûtement*, Bibliothèque d'Étude 101, Cairo.

Pozza G., Ajo D., Chiari G., De Zuane F. and M.L. Favaro (2000), 'Photoluminescence of the inorganic pigments Egyptian blue, Han blue and Han purple', *Journal of Cultural Heritage* 1, 393-398. DOI: 10.1016/S1296-2074(00)01095-5

Quack, J. F. (2002), 'Some Old Kingdom Execration Figurines from the Teti Cemetery', *Bulletin of the Australian Centre for Egyptology* 13, 149-163.

Remondino, F. (2011), 'Advanced 3D Recording Techniques for the Digital Documentation and Conservation of Heritage Sites and Objects', *Change Over Time* 1/2, 198–214.

Ritner, R.K. (1993), *The Mechanics of Ancient Egyptian Magical Practice*, Studies in Ancient Oriental Civilization 54, Chicago.

Scott D. A. (2010), 'Greener shades of pale: a review of advances in the characterisation of ancient Egyptian green pigments', in: Dawson J., Rozeik C and M.M. Wright (eds.), *Decorated Surfaces on Ancient Egyptian Object: Technology, Deterioration and Conservation*, London, 32-45.

Serotta, A. (2010), Aspects of the Technical Analysis of an Egyptian Relief from the Metropolitan Museum of Art, Poster IIC 2010 Istanbul Congress: Conservation and the Eastern Mediterranean.

Sethe, K. (1926), *Die Ächtung feindlicher Fürsten, Völker und Dinge auf altägyptischen Tongefässscherben des Mittleren Reiches*, Berlin.

Theis, C. (2014), *Magie und Raum*, Orientalische Religionen in der Antike 13, Tübingen.

Thompson, D.V. and G.H. Hamilton (1933), *De arte illuminandi: the technique of manuscript illumination, an anonymous 14th-century treatise*, New Haven, Connecticut.

Tite M., Bimson M. and M.R. Cowell (1987), 'The Technology of Egyptian Blue', in: Bimson M. and I.C. Freestone (eds.), *Early Vitreous Materials*, London, 19-47.

Toth, R. B. (2015) Applying New Technologies to Cultural Studies. Website R.B. Toth Associates [online]. Available from: <http://www.rbtoth.com/> [Accessed 12th November 2015].

Trentelman, K., Schmidt Patterson, C. and N. Turner (2012), XRF analysis of manuscript illuminations, in: Shugar, A.N and J.L. Mass, *Handheld XRF for Art and Archaeology*, Leuven, 159-189.

Van de Walle, B., Limme, L. and H. De Meulenaere (1980), *La collection égyptienne. Les étapes marquantes de son développement*, Brussels.

Van der Perre, A. and H. Hameeuw (2015), 'La création d'images multi-spectrales: les portraits romains du Fayoum', in : Delvaux, L. and I. Therasse (eds), *Sarcophages. Sous les étoiles de Nout*, Brussels, 164-165.

Van der Perre, A., Hameeuw, H., Boschloos, V., Delvaux, L., Proesmans, M., Vandermeulen B., Van Gool, L. and L. Watteeuw (2016), 'Towards a combined use of IR, UV and 3D-imaging for the study of small inscribed and illuminated artefacts', in: P. M. Homem (ed.), *Lights On... Cultural Heritage and Museums!*, Porto, 163-192.

Van der Perre, A., Braekmans, D., Boschloos, V., Ossieur F., Hameeuw, H. and L. Delvaux, 'The Egyptian Execration Figurines of the Royal Museums of Art and History, Brussels: Conservation, Pigments and Digitisation', *Bulletin des Musées royaux d'Art et d'Histoire, Bruxelles* 85 (2014) (in press).

Verbiest, F. and L. Van Gool (2008), 'Photometric stereo with coherent outlier handling and confidence estimation', in: *Proceedings IEEE Conference on Computer Vision and Pattern Recognition*, June 24-26, 2008, New York, 2886-2893.

Verri G. (2009a), 'The spatially resolved characterization of Egyptian blue, Han blue and Han purple by photo-induced luminescence digital imaging', *Analytical and bioanalytical chemistry* 394/4, 1011-1021. DOI:10.1007/s00216-009-2693-0

Verri G. (2009b), 'The application of visible-induced luminescence imaging to the examination of museum objects', in: *Proceedings of SPIE - The International Society for Optical Engineering* 7391 - July 2009, 1-12. DOI:10.1117/12.827331

Verri G., Saunders D., Ambers J. and T. Sweek (2010), 'Digital mapping of Egyptian blue: Conservation implications', *Studies in Conservation* 55 (Supplement-2), 220-224.

Watteeuw, L. and M. Van Bos (2010), 'Illuminating with Pen and Brush. The Techniques of a Fourteenth-Century Neapolitan Illuminator Explored', in: Watteeuw L. and J. Van der Stock (Eds.), *The Anjou Bible. Naples 1340. A Royal Manuscript Revealed*, Corpus of Illuminated Manuscripts, vol. 18, Leuven, 147-170.

Watteeuw, L., Vandermeulen, B., Van der Stock, J., Delsaerdt, P., Gradmann, S., Truyen, F., Proesmans, M., Moreau, W. and L. Van Gool (2013), 'Imaging Characteristics of Graphic Materials with the Minidome (RICH)', in: *Paper Conservation. Decisions & Compromise. ICOM-CC graphic documents working group interim meeting. Vienna, Austria, 17-19 April 2013*, Vienna, 140-141.

Watteeuw, L., Hameeuw, H., Vandermeulen, B., Van der Perre, A., Boschloos, V., Delvaux, L., Van Bos, M., Proesmans, M. and L. Van Gool (2016), Light, Shadows and Surface Characteristics. The Multispectral Portable Light Dome, *Applied Physics A* 122: 976, 1-7.

Willems G., Verbiest F., Moreau W., Hameeuw H., Van Lerberghe K. and L. Van Gool (2005), 'Easy and Cost-Effective Cuneiform Digitizing', in: Mudge M., Ryan N. and R. Scopigno (eds.), *The 6th International Symposium on Virtual Reality, Archaeology and Cultural Heritage (VAST 2005)*, Pisa, 73-80.

Wodzinska, A. (2009), *A Manual of Egyptian Pottery. Vol. 2: Naqada III-Middle Kingdom*. Ancient Egypt Research Associates Field Manual Series 1, Hollis.

Woodham, R.J. (1980), 'Photometric method for determining surface orientation from multiple images', *Optical Engineerings* 19(1), 139-144.

ANNEXES

Annexe 1: Origin and Dispersion of the Brussels Execration Figurines

As is often the case with objects circulating on the antiquities market, the origin of the figurines was not exactly known. The French Egyptologist Georges Posener, however, studied a similar group of figurines at the Cairo Museum, prior to the acquisition of the Brussels group (Posener 1939: 39-46). The provenance of the Cairo figurines was well known, being discovered during the excavations of Cecil M. Firth at Saqqara in 1922, in the vicinity of the Teti Pyramid. Similar figurines can be seen on the photo of Hakin Abu Seif (Posener 1940: Fig. 2), made during the excavation of the rectangular, mud brick construction located to the north of the Teti pyramid wall. The structure was not described in the publication of the excavation, but is marked in the south-eastern corner of the sketch plan of the site (Firth and Gunn 1926: pl. 51). It was dated to the early Middle Kingdom and contained five decorated stelae and five offering tables. Since no burials were related to it, the structure was identified as a cenotaph, belonging to the family of Sekwaskhet (Abdalla 1992: 93-111). The precise location of the figurines within this construction is not known. According to the inspector of the Service des Antiquités de Saqqara, the figurines were found “*sur le dallage dans une enveloppe de terre*” in the north-eastern part of the structure. The figurines were briefly studied by Battiscombe G. Gunn in 1925, as is confirmed by one of his personal notebooks currently stored in the Griffith Archives at Oxford (Gunn MSS 29: Clay Figures I. 1925. Transcriptions). They were stored in the excavation storeroom at Saqqara, until the spring of 1938, when they were transferred to the Cairo Museum by the director of the Antiquities Service Étienne Drioton. Posener briefly studied them during this period. Due to their similarity with the Cairo figurines in both appearance and content, it was suggested that the Brussels group also originated from this location. This was later confirmed by Posener, who was able to join pieces from both collections (Posener 1987: 3). It is clear that the Brussels group was actually stolen at some point from the storeroom at Saqqara between 1925 and 1938. On one of the excavation photos of Gunn (Gunn MSS XIV 40[3]), the Brussels figurine E.7446 is depicted, clearly proving that the origin of the Brussels groups was in fact Saqqara.

Soon after their arrival in the RMAH, the original Brussels Group was dispersed. A representative collection was kept in the museum and registered upon arrival under the numbers E.7440 – E.7494. The remaining figurines were divided into five batches (dubbed Lot A – E) with the intention to sell these to other public collections abroad, for the price of 10.000 Belgian francs per Lot. The Leiden *Rijksmuseum van Oudheden* (RMO) acquired Lot C, containing twelve figurines, in 1941 (Former N° 2, 17, 23, 30, 37, 46, 56, 76, 83, 91, 97 and 104. Now registered as Leiden F.1941/8.1-F.1941/8.12). Lot D eventually went to the Eretz Israel Museum in Tel Aviv. It originally contained twelve figurines, but for an unknown reason, it was decided to keep four of them in Brussels (E.7612, E.7613, E.9060 and E.9082). The remaining eight figurines were nevertheless exchanged for a batch of finds from different

sites in Palestine (Former N° 42, 45, 58, 92, 102, 113, 115 and 119). Lot E was destined for the Cairo museum, containing the fragments that join with the Cairo figurines.

Lot E and the other series eventually did not leave the museum, and were registered in two phases. In January 1942, eight figurines were added to the inventory of the museum under the numbers E.7607 – E.7614. The remaining figurines entered the museum catalogue in 1995 with E.9000 inventory numbers (E.9060 - E.9100), even though they were “rediscovered” in the storeroom around 1982. This last group contains five (fragments of) figurines that were donated by Khawam to the *Fondation Égyptologique Reine Élisabeth*. They were donated to the museum in 1946, together with a group of other Egyptian objects, when they received a preliminary inventory number (E.7649a - e). However, in 1995 they were renumbered E.9096-E.9100.

Annexe 2: Condition Assessment Form

CONDITION REPORT EXECRATION FIGURINES

Date:
France Ossieur Assisted by: Athena Van der Perre Vanessa Boschloos
Examination technique
<input type="radio"/> Visual (v) <input type="radio"/> Magnified (ma) <input type="radio"/> Microscope (mi)

Inv. Nr. E.	Photo
Present location :	
General condition: <input type="radio"/> Appears stable/sound <input type="radio"/> Active deterioration noticed <input type="radio"/> Damage noted <input type="radio"/> Fragile/weak	Form: <input type="radio"/> Intact <input type="radio"/> Broken / fragmented pieces <input type="radio"/> Incomplete

Condition			
External/Surface	Slip – Wet finishing <input type="radio"/> Front <input type="radio"/> Back <input type="radio"/> Right side <input type="radio"/> Left Side <input type="radio"/> All sides <input type="radio"/> Cannot be determined	Cohesion: <input type="radio"/> Good <input type="radio"/> Bad <input type="radio"/> Problematic <input type="radio"/> ...	<input type="radio"/> Holes <input type="radio"/> Cracks <input type="radio"/> Crazing <input type="radio"/> Flaking <input type="radio"/> Friable <input type="radio"/> Abrasion <input type="radio"/> Loss <input type="radio"/>
	Colour:	<input type="radio"/> Dusty <input type="radio"/> Salts/Perspiration <input type="radio"/> Discoloured <input type="radio"/> Stains/spots	
	Remarks:		
Inscriptions	Location: <input type="radio"/> Recto <input type="radio"/> Verso <input type="radio"/> Head <input type="radio"/> Knees <input type="radio"/> Left side <input type="radio"/> Right side	Colour: <input type="radio"/> Black <input type="radio"/> Red ochre <input type="radio"/> Ochre <input type="radio"/> ...	Condition: <input type="radio"/> Discoloured <input type="radio"/> Faded <input type="radio"/> Well preserved <input type="radio"/> ...
	Remarks:		

Interior	Material: <input type="radio"/> Unfired clay <input type="radio"/> Nile silt <input type="radio"/> Marl <input type="radio"/> ...	Cohesion: <input type="radio"/> Good <input type="radio"/> Bad <input type="radio"/> Problematic <input type="radio"/> ...	Cohesion with surface layer: <input type="radio"/> Good <input type="radio"/> Bad <input type="radio"/> Problematic <input type="radio"/> Not applicable
	Inclusions: <input type="radio"/> Mineral (quartz, feldspar, sand,...) <input type="radio"/> Organic material <input type="radio"/> Crushed sherds <input type="radio"/> Shells/fossils <input type="radio"/> Mica <input type="radio"/> Grey white gran. <input type="radio"/> ...	Condition: <input type="radio"/> Holes <input type="radio"/> Cracks <input type="radio"/> Friable <input type="radio"/> Loss <input type="radio"/> Crazing	<input type="radio"/> Dusty <input type="radio"/> Salts/Perspiration <input type="radio"/> Discoloured <input type="radio"/> Stains/spots <input type="radio"/> ...
	Description:		
	Remarks:		

Surface treatments		
Previous consolidation treatments <input type="radio"/> Yes <input type="radio"/> No	Submersed in paraxylene + paraloid B72: <input type="radio"/> Yes <input type="radio"/> Probably <input type="radio"/> Possibly <input type="radio"/> Probably not <input type="radio"/> No	Other:
	Remarks:	
Previous restoration / repairs <input type="radio"/> Yes <input type="radio"/> No	Type: <input type="radio"/> Reassembled <input type="radio"/> Dry-cleaned <input type="radio"/> Wet-cleaned <input type="radio"/> Additions/alterations <input type="radio"/> Filled <input type="radio"/> ...	Products: <input type="radio"/> Glue: <input type="radio"/> Clay <input type="radio"/> ...
	Remarks:	
Restoration files	<input type="radio"/> Yes: <input type="radio"/> No	

Annexe 3: WDXRF – RMAH (E.7444)

Experimental conditions:

For XRF analysis the measurements were performed with a Panalytical Axios Max WD-XRF data evaluation was done with SuperQ5.0i/Omnian software. 18/12/2015 09:37:03 spectrometer and

All 38 samples:

Binder
Chemical formula Weight (g)
C18H36O2N2 0.5

03/11/2016 14:59:49

PANalytical

Quantification of sample D. Braekmans, sample 1. 31oct16

Sum before normalization: 90.7 wt%

Normalised to: 100.0 wt%

Sample type: Pressed powder

Initial sample weight (g): 2.000

Weight after pressing (g): 2.500

Oxygen validation factor: 0.93

Correction applied for medium: No

Correction applied for film: No

Used Compound list: Oxides

Results database: omnian 4kw 27mm

Results database in: c:\panalytical\superq\userdata

03/11/2016 15:18:14

PANalytical

Quantification of sample D. Braekmans, sample E.7444. 28oct16

Sum before normalization: 63.8 wt%

Normalised to: 100.0 wt%

Sample type: Pressed powder

Initial sample weight (g): 2.000

Weight after pressing (g): 2.500

Oxygen validation factor: 0.00

Correction applied for medium: No

Correction applied for film: No

Used Compound list: Oxides

Results database: omnian 4kw 27mm

Results database in: c:\panalytical\superq\userdata

	Compound Name	Conc. (wt%)	Absolute (Ewrtr%or)
1	SiO2	53.053	0.1
2	Al2O3	15.221	0.1
3	Fe2O3	13.7	0.1
4	CaO	5.518	0.07
5	MgO	3.253	0.05
6	TiO2	2.176	0.04

7	Na ₂ O	1.957	0.04
8	P ₂ O ₅	1.894	0.04
9	K ₂ O	1.26	0.03
10	Cl	0.776	0.03
11	SO ₃	0.584	0.02
12	MnO	0.185	0.01
13	BaO	0.12	0.01
14	ZnO	0.082	0.009
15	SrO	0.074	0.008
16	ZrO ₂	0.058	0.007
17	NiO	0.034	0.006
18	Cr ₂ O ₃	0.023	0.005
19	CuO	0.017	0.004
20	Rb ₂ O	0.008	0.003
21	Nb ₂ O ₅	0.005	0.002